Luminogenic polymers with aggregation-induced emission characteristics

Anjun Qin[a], Jacky W.Y. Lam[b,c], Ben Zhong Tang[a,b,c,*]

[a] MOE Key Laboratory of Macromolecular Synthesis and Functionalization, Department of Polymer Science and Engineering, Zhejiang University, Hangzhou 310027, China
[b] Department of Chemistry, Institute of Molecular Functional Materials, The Hong Kong University of Science and Technology (HKUST), Clear Water Bay, Kowloon, Hong Kong, China
[c] HKUST Fok Ying Tung Research Institute, Nansha, Guangzhou, China

ARTICLE INFO

ABSTRACT

Aggregation-induced emission (AIE) is a newly developed phenomenon that is exactly opposite to the aggregation-caused emission quenching effect observed with some conventional luminophores. The AIE phenomenon was first realized in propeller-like small molecules and now has extended to polymeric systems. In this review, we summarize the recent progress on the preparation of luminogenic polymers with AIE or aggregation-enhanced emission (AEE) characteristics, which are generally prepared by attaching AIE-active luminogens, such as tetraphenylethene and silole, as pendants to the polymer backbones or utilizing them as skeletons for main chain polymers. An AIE phenomenon was observed in succinic anhydride-containing nonconjugated polymers bearing no luminogens, presumably due to the agglomeration of carbonyl groups. The AIE/AEE-active polymers show unique properties, such as emission superquenching, high and tunable light refractivity, and aggregation-enhanced two-photon excited fluorescence, and have found potential applications as fluorescent sensors, biological probes, and active layers for the fabrication of light-emitting diodes.

Contents

1. Introduction

Organic and polymeric luminophores are promising materials for applications in various areas, such as light-emitting diodes [1–6], plastic lasers [7–9], and fluorescent chemosensors and bioprobes [10–16]. To respond to the demand, scientists have synthesized a large number of luminescent materials. Many of them have been found to be highly emissive in dilute solutions, with fluorescence quantum yields reaching unity. For most practical applications, the luminescent materials have to be used in the solid state (e.g. as thin films), where the luminophores tend to form aggregates. However, it is known that aggregation of organic luminophores often leads to partial or even complete quenching of their light emissions. This aggregation-caused quenching (ACQ) effect has limited the scope of technological applications of the luminophoric molecules. To alleviate the ACQ effect in the condensed phase, various chemical, physical, and engineering approaches have been developed. For example, branched chains, bulky cyclics, spiro kinks, and dendritic wedges have been covalently attached to aromatic rings to impede aggregate formation [17–28]. Luminogens have also been physically passivated via surfactant encapsulation, doped into matrices of nonconjugated transparent polymers such as poly(methyl methacrylate), and blended with different inorganic or organic or polymeric materials [29–34]. Although various approaches have been taken to interfere with luminogen aggregation, the attempts have met with only limited success and they, however, are often accompanied by severe side effects. The steric effects of bulky cyclics, for example, can twist the conformations of the chromophoric units and thus partially jeopardize the electron conjugation in the luminophores. The nonconjugated encapsulates and the transparent matrices used in the physical processes are nonemissive and insulating, and can dilute the luminophore density and obstruct the charge

transport in electroluminescence (EL) devices. The spatial distribution of the fluorophore dopants in a doped film suffers from temporal instability: the luminogens dispersed in the polymer matrices gradually migrate together over time, eventually emerging phase separation and forming large aggregates [2].

As aggregation is an inherent process when luminogenic molecules are in the condensed phase, it would be useful to develop a system in which aggregation plays a constructive, rather than destructive role, in the light-emitting processes of luminogens [35–51]. In their search for efficient luminescent materials, Tang and co-workers were attracted by a group of organometallic molecules called siloles. A silole molecule named hexaphenylsilole (HPS or **1**) is shown in Fig. 1 as an example, whose electronic structure looks extensively conjugated. However, the silole molecules were found to be virtually non-luminescent when molecularly dissolved in good solvents, but became highly emissive when aggregated in poor solvents or fabricated into thin solid films. They coined the term of "aggregation-induced emission (AIE)" for this phenomenon because the silole molecules were induced to emit by aggregate formation [52,53]. Since then, many organic fluorogens have been found to show the AIE effect [54–62] and behave like HPS. For example, a dilute THF solution of tetraphenylethene (TPE or **2**) is practically non-luminescent (Fig. 1), but addition of a poor solvent, such as water, induces aggregation and results in light emission.

Some luminogenic materials exhibit "turn-on" photophysical properties when utilized as chemo- and biosensors due to metal complexation, hydrogen-bond formation, electrostatic interaction, chemical reaction, etc. [63–66]. What is the working principle for the AIE effect? A number of possible mechanistic pathways, including conformational planarization, J-aggregate formation, twisted intramolecular charge transfer (TICT), and restriction of intramolecular rotation (RIR), have been proposed for
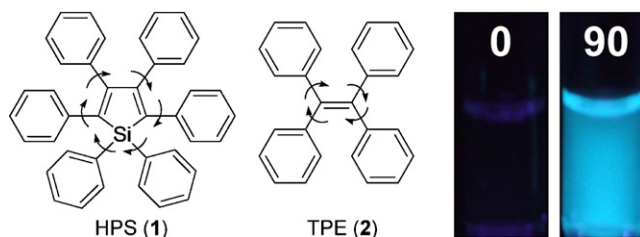

Fig. 1. Molecular structures of HPS and TPE and fluorescent images of TPE in THF/water mixtures with water fractions of 0 and 90%. The bright rim at the top of the blue image is caused by an optical effect due to the container. (For interpretation of the references to color in this figure legend, the reader is referred to the web version of the article.)

the AIE phenomenon. Through a series of externally and internally modulated experiments and theoretical studies [67–79], Tang and co-workers rationalized that RIR is the main cause for the AIE effect of their systems [62,79]. According to fundamental physics, any molecular motion will consume energy. As depicted schematically in Fig. 1, the phenyl rings of HPS and TPE can undergo dynamic intramolecular rotations against the silole and olefin cores. In the solution state, such rotation is active, which serves as relaxation channel for the excited state to decay. Whereas, in the aggregated state, this rotation is restricted due to physical constraints on the molecular packing, blocking the nonradiative path and activates the radiative decay.

Most of the AIE systems developed so far are low-molecular-weight molecules. For practical applications, the luminogens have to be fabricated into thin solid films by expensive techniques, such as vacuum sublimation and vapor deposition, which are not well suited to the manufacture of large-area flat-panel devices. One way to overcome this processing disadvantage is to make polymers, which have high molecular weight and good film-forming capacity, and can be fabricated into large-area thin solid films and devices at ambient conditions by simple processes such as spin-coating, static casting, and ink-jet printing [80].

Conjugated polymers have been utilized in light-emitting diodes, fluorescent chemosensors and bioprobes, and solid-state lasers. Some of them, however, also encounter the ACQ problem in the condensed phase, which has consequently decreased their device performances. Preparation of linear and hyperbranched polymers with AIE or aggregation-enhanced emission (AEE) features may help to solve the problem and meanwhile impart polymers with new properties and practical applications. Although the research on this topic is still in its infancy, many works with excellent results have been achieved. In this review, we will summarize the recent progress on the preparation of AIE/AEE-active linear and hyperbranched polymers and their potential applications.

2. Polyacetylenes

As evidenced by the 2000 Nobel Prize in Chemistry, polyacetylene is an archetypal conjugated polymer [81–83] and exhibits a metallic conductivity upon doping. Little work has been done on the development of light-emitting polyacetylenes because the pristine polymers are non-luminescent. Replacement of the hydrogen atoms in its repeat units by appropriate substituents can fine-tune its electronic properties and generate mono- and disubstitued polyacetylenes [84–86]. During the course of exploiting alkyne polymerizations and developing alkynes into a group of versatile building blocks for the construction of new polymers with linear and hyperbranched structures and advanced functional properties [87–89], Tang and co-workers found that some disubstituted polyacetylenes such as poly(diphenylacetylene)s (PDPAs) and poly(1-phenyl-1-alkyne)s (PPAs) (Fig. 2), with pendant phenyl (or phenylene) rings on the main chains, are structurally similar to those on TPE. In TPE, the hydrogen atoms of its olefin core are replaced by four phenyl rings, while
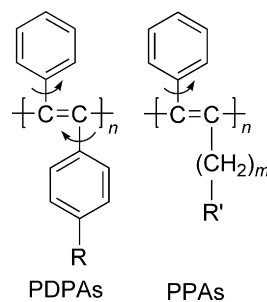

Fig. 2. Molecular structures of disubstituted polyacetylenes.

in disubstituted polyacetylenes, every monomer unit has two or one phenyl rings linked to the central vinyl core. Thus, the mechanism for their emission enhancement in the aggregate state should be similar and can be ascribed to the RIR process.

Fig. 3 shows the photoluminescence (PL) spectra of PDPA **3** and PPA **4** in THF/water mixtures with 0 and 90% water fractions (f_w) as examples. Polymer **3** emits green light at 506 nm in THF. Its spectrum contains no fine structure and is very broad with a full width at half-maximum (fwhm) as large as ∼107 nm, characteristic of the emission from intramolecular excimers governed by the "$n = 3$" rule (Fig. 3A) [90,91]. According to this rule, molecules with phenyl rings spatially separated by 3 carbon atoms (e.g. 1,3-diphenylpropane and polystyrene) can form intramolecular excimers that emit in the redder spectral regions, compared to their "monomer" emission. The trans-transoid conformation in the chain segments of **3** meets the "$n = 3$" rule for the formation of intramolecular excimers, and is seen to emit at the longer spectral region [92,93]. The addition of water into the THF solution of **3** has generally increased its emission. Meanwhile, its PL spectra are bathochromically shifted by ∼25 nm in the aqueous mixtures with high f_w. Since the polymer is insoluble in water, the shrinkage in the molecular volume accompanying the aggregate formation in the aqueous mixture physically puts the phenyl rings in closer vicinities. This enhances the π-stacking interactions of the phenyl rings and restricts their intramolecular rotations: the former red-shifts the emission spectrum, while the latter boosts its emission intensity. Polymer **4** shares a similar spectral profile with an fwhm of ∼95 nm. It emits blue light in THF and exhibits no peak shifts when aggregated in aqueous mixtures (Fig. 3B). The emission of **4** in 90% aqueous mixture is ∼2-fold stronger than that in THF, revealing its AEE characteristic [92–94].

Unlike PDPAs and PPAs, monosubstituted polyacetylenes carrying no luminophoric units are nonluminescent but can be imparted with AIE or AEE features by attaching AIE luminogens to their polymer backbones. Tang and co-workers worked on the synthesis of monosubstituted polyacetylenes with silole and TPE pendant groups and studied the dependence of the optical properties of the polymers on their molecular structures (Fig. 4) [95,96]. They found that the chloroform solution of **5** emits faint red light from the polymer backbone at 652 nm. No bluish-green emission from the silole pendant was observed.
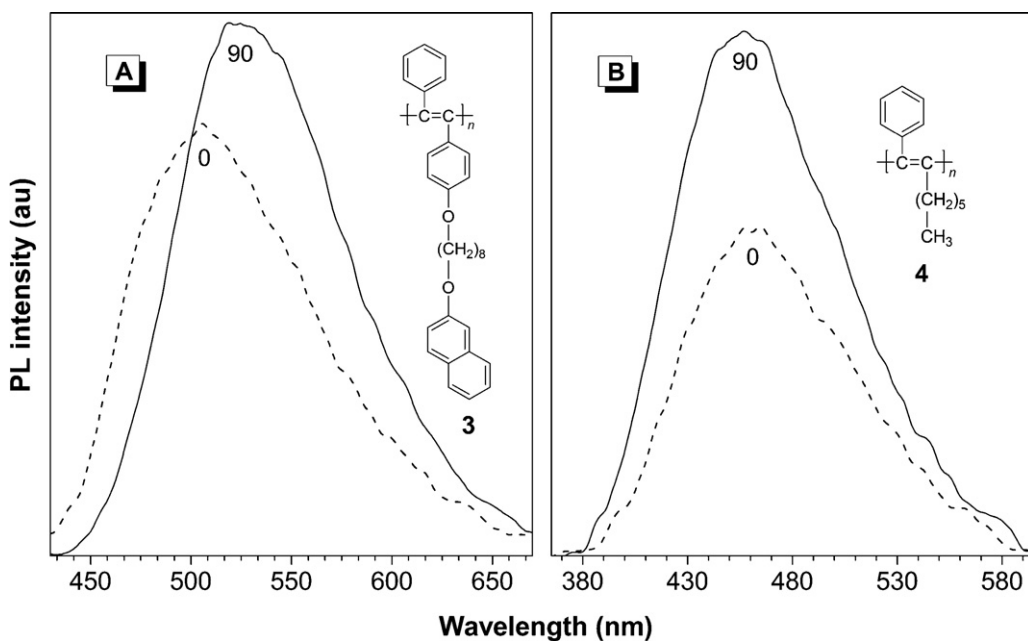
Fig. 3. PL spectra of AEE-active disubstituted polyacetylenes **3** and **4** in THF solutions and THF/water mixtures with 90% water contents. Reprinted with permission from Ref. [92].
© 2008, American Chemical Society.

Addition of a poor solvent such as methanol into its THF solution slightly increased the emission, demonstrating that **5** is AIE-inactive. The rigid polyacetylene strands of **5** may not allow the directly attached silole pendants to pack well in the aggregate state, thus showing no AIE phenomenon. In contrast, polyacetylene with directly attached TPE derivative (**6**) is AEE-active: it shows weak luminescence peaked at 613 nm in THF due to the conjugation of the TPE pendants with the polymer backbone. The emission

intensity is enhanced when the polymer strands aggregate in the presence of water. The maximum PL increment is ~2.8-fold.

Although the direct attachment of AIE luminogens to the polyacetylene backbone facilitates better electronic communication, it also favors exciton trap by the structural defects in the polymer skeleton, and hence lowers the emission efficiency significantly. Insertion of a flexible alkyl spacer between the polymer backbone and
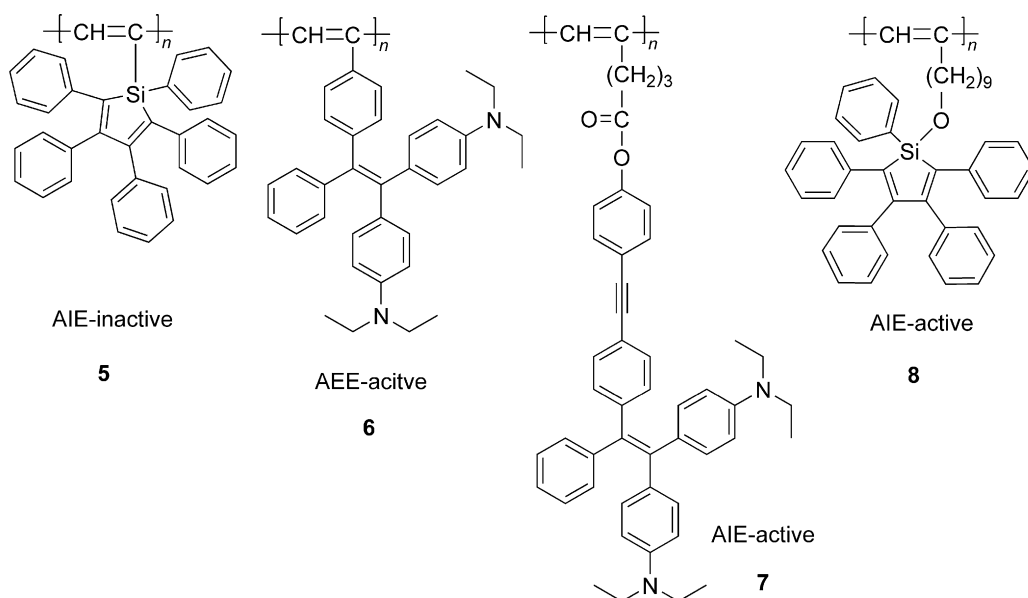

Fig. 4. Molecular structures of silole and TPE-containing monosubstituted polyacetylenes [95,96].
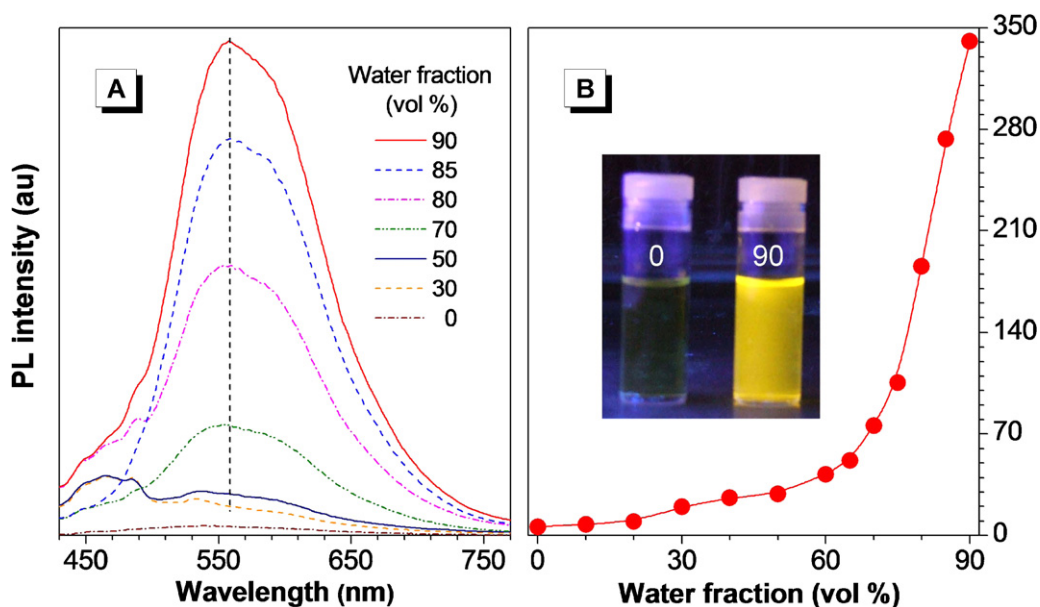
Fig. 5. (A) PL spectra of **7** in THF/water mixtures with different water fractions. (B) Variation of emission intensity of **7** at 588 nm with water fraction in the THF/water mixture. Inset: photographs of **7** in THF and THF/water mixture with 90% water content.
Reprinted with permission from Ref. [96].
© 2009, American Chemical Society.

the pendant group makes the resultant polymers **7** and **8** AIE-active because their pendants can undergo intramolecular rotation in solution [79]. As demonstrated in Fig. 5A, **7** is practically nonluminescent when molecularly dissolved in good solvents and its PL spectrum in dilute THF solution is almost a flat line parallel to the abscissa. However, a strong PL signal was recorded under the same experimental conditions when a large amount of water was added into its THF solution. The emission gradually intensified with increasing f_w in THF/water mixtures. The enhancement increases rapidly with increased water content for $f_w > 75\%$ (Fig. 5B). At $f_w = 90\%$, the intensity is more than 56-fold higher than that in THF. Similarly, the chloroform solution of **8** emits faintly with a fluorescence quantum yield (Φ_F) as low as 0.2%. The Φ_F value rises by ~20-fold to 3.0% in chloroform/methanol mixture with 90% methanol fraction (f_m), displaying a typical AIE behavior.

Polymer **9**, a disubstituted counterpart of **8**, is also AIE-active (Fig. 6). Its THF solution is almost nonluminescent, but its aggregates in 90% aqueous mixture emit intensely with ~46-fold higher intensity at 512 nm. As poly(1-phenyl-1-octyne) emits at ~460 nm in the aggregate state, the peak observed at 512 nm in the aggregates of **9** is thus believed to be originated from the emission of its silole pendants. The Φ_F value of **9** (9.3%) is more than three times higher than that of **8**, probably due to the additional contribution from the emissive polymer backbone.

The EL of **9** was also investigated by fabricating a multilayer EL device with a configuration of ITO/**9**:PVK(1:4)/BCP/Alq$_3$/LiF/Al, where ITO: indium-tin oxide, PVK: poly(9-vinylcarbazole) (hole-transporting layer), BCP: bathocuproine (hole-blocking layer), and Alq$_3$: tris(8-hydroxyquinolinato)aluminum (electron-transporting layer). The EL spectrum of **9** peaks at 496 nm and is close

to the PL peak of its aggregates, verifying that the EL is stemmed from the silole unit. The maximum luminance, current efficiency, and external quantum efficiency attained by the device are 1118 cd/m^2, 1.45 cd/A, and 0.55%, respectively (Fig. 6), which can be enhanced by further modifying the molecular structure of the polymer and optimizing the configuration of the EL device.

Taking advantage of the AEE effect, bright fluorescent 3D patterns can be generated from PDPAs containing
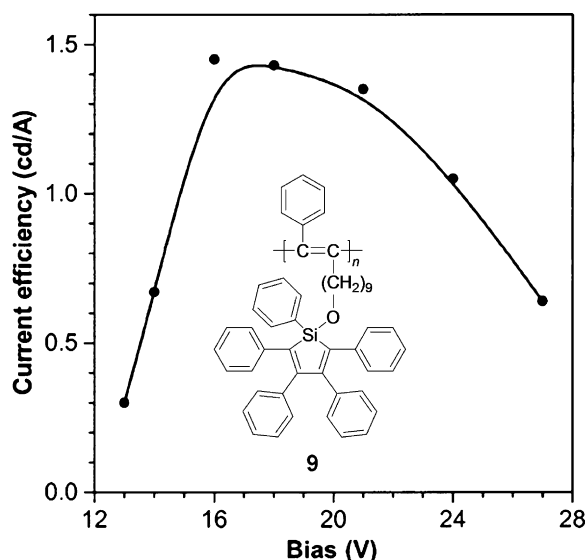

Fig. 6. Current efficiency vs. applied bias in a multilayer electroluminescence device of **9** with a configuration of ITO/**9**:PVK(1:4)/BCP/Alq$_3$/LiF/Al. Reprinted with permission from Ref. [95].
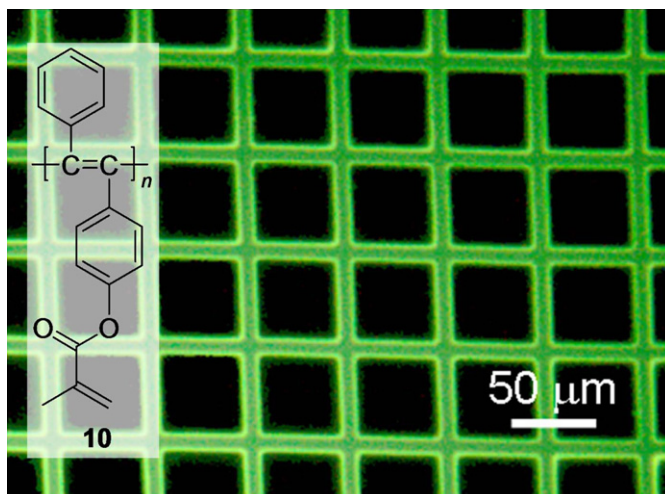© 2003, American Chemical Society.

Fig. 7. Fluorescent photopattern generated by photo-cross-linking of **10**. The picture was taken under UV illumination.
Reprinted with permission from Ref. [93].
© 2007, American Chemical Society.

cross-linkable groups. It is well known that materials with (meth)acrylate moiety cross-link readily upon UV irradiation. Thus, UV irradiation of a thin film of **10** through a copper mask cross-links the uncovered parts, whereas the covered parts remain soluble. A three-dimensional fluorescent negative photoresist pattern is generated after development, which gives strong green light when observed under a fluorescent microscope (Fig. 7).

The detection of biopolymers by polyelectrolytes is emerging as an active and critical area of research because it plays an important role in biological science and engineering [97–100]. Polymer **7** can be converted into water-soluble conjugated polyelectrolyte by hydrochloric acid owing to the transformation of its diethylamino group to an ammonium salt. Quaternized **7** is also AIE-active and shows a high affinity to negatively charged biopolymers, such as bovine serum albumin (BSA). As depicted in Fig. 8, the emission of quaternized **7** in aqueous buffer solution is progressively intensified with gradual addition of BSA due to the RIR process. The detection threshold can be down to sub-ppm, and at a BSA concentration of 20 μg/mL, the emission intensity is increased by ~7.5-fold. Clearly, quaternized **7** can function as a turn-on bioprobe.

3. Polyphenylenes

Hyperbranched polymers have drawn much attention in recent years because they enjoy the advantages of readily synthetic access, unique molecular structure, microscopic processibility, and periphery functionalization, etc. [101–103]. Tang and co-workers worked on the preparation of hyperbranched polyphenylenes with AIE/AEE features [104,105]. They first investigated the silole-containing poly(1,1-silolylphenylene) **13**. The polymer was synthesized in a high yield via Ta-catalyzed polycyclotrimerization of 1,1-diethynyl-2,3,4,5-tetraphenylsilole (**11**), an A_2-type monomer, in the presence or absence of monoyne **12** (Fig. 9) [106]. Although the Φ_F value is low (1.0%), the polymer is emissive and gives a blue-green

light at ~500 nm when its dilute THF solution is irradiated. However, instead of being intensified, its emission is weakened when its chains are aggregated in methanol, a poor solvent for the polymer, illustrating that **13** is AIE-inactive. On the contrary, its PL is enhanced when its dilute dioxane solution is cooled, displaying a cooling-enhanced emission characteristic. Such phenomena are associated with the sterically crowded structure of the polymer, which partially restricts the motion of the phenyl rings and thus renders the polymer emissive in the solution. On the other hand, the chaotic stacks of the rigid polymer chains in the
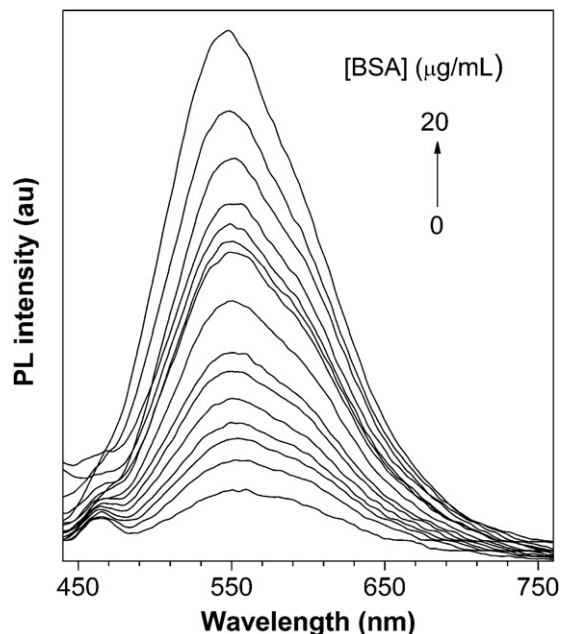

Fig. 8. PL spectra of quaternized **7** in aqueous phosphate buffers containing different amounts of BSA.
Reprinted with permission from Ref. [96].
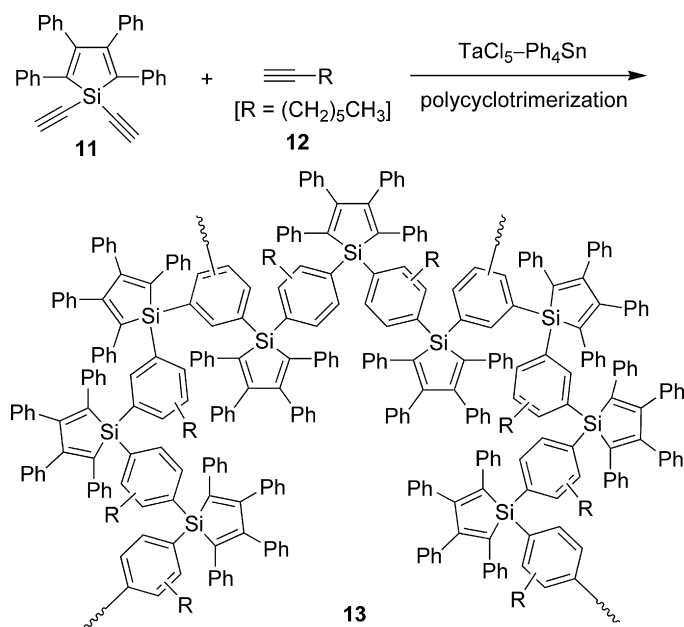© 2009, American Chemical Society.

Fig. 9. Preparation of hyperbranched poly(1,1-silolylphenylene) **13** [106].

aggregate state may generate large free volume, in which the phenyl rings may still be able to rotate. Such inter- and intra-molecular interactions may have nonradiatively deactivated the excited species and hence quenched the polymer emission.

By varying the linkage site from 1,1- to 2,5-positions, the resultant hyperbranched poly(2,5-silolylphenylene)s

are less sterically hindered [70,105,107]. Fig. 10 shows an example of such polymer (**15**) prepared by Ta-mediated homopolycyclotrimerization of 1,1-dihexyl-2,5-bis(4-ethynylphenyl)-3,4-diphenylsilole (**14**).

Although **14** is nonemissive in dilute solution, its poly-mer **15** is already somewhat luminescent due to the activation of the RIR process via knitting the rotary phenyl
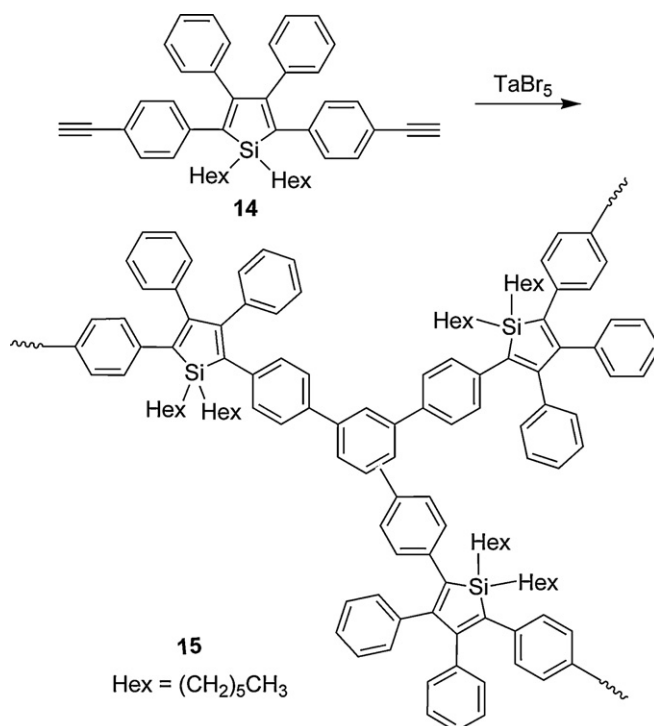

Fig. 10. Synthesis of AEE-active hyperbranched poly(2,5-silolylphenylene) **15** by diyne homepolycyclotrimerization [107].

units by the rigid polymer skeleton. Different from polymer **13**, **15** is AEE-active (Fig. 11): gradual addition of water into its THF solution has progressively enhanced its light emission. These results thus provide valuable information on the relationship between the polymer structure and the AIE phenomenon.

Realizing that steric effects play a crucial role in generating hyperbranched polymers with AIE/AEE characteristics, Tang and co-workers further introduced a more flexible node such as silicon atom into the polymer branches. The σ^*–π^* conjugated hyperbranched poly(silylenephenylene) (**17**) was synthesized in a high yield (up to 100%) by Ta-catalyzed polycyclotrimerization of silylenediyne **16** (Fig. 12) [108]. The polymer emits UV light (~380 nm) in dilute solution with a Φ_F value of ~7%. When water is added, nanoaggregates of **17** are formed, which emit at the same spectral region but with higher intensity. The Φ_F value (~23%) of the polymer solid film is much higher than that in the THF solution, demonstrative of its AEE characteristic. As shown in the inset of Fig. 12, the triphenylbenzene (TPB) repeat units possess three freely rotary phenyl rings, whose motions will quench the PL of the polymer in the solution state. On the other hand, the RIR process is activated when the polymer forms aggregate in aqueous mixtures, which consequently enhances its light emission [109,110].

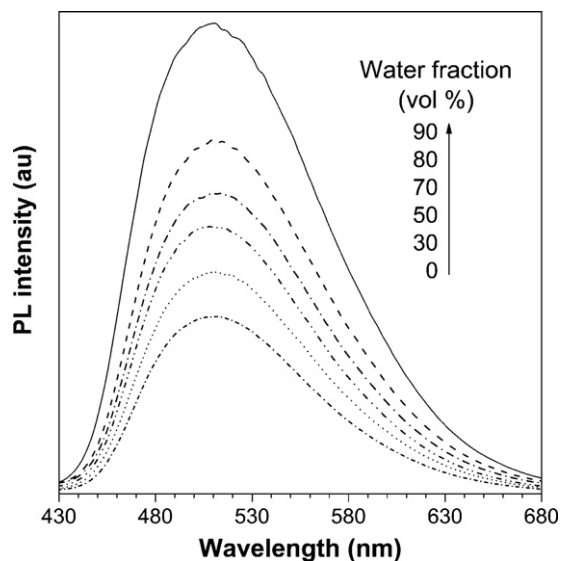**Fig. 11.** PL spectra of **15** in THF/water mixtures with different water fractions per the data in panel B.
Reprinted with permission from Ref. [107].
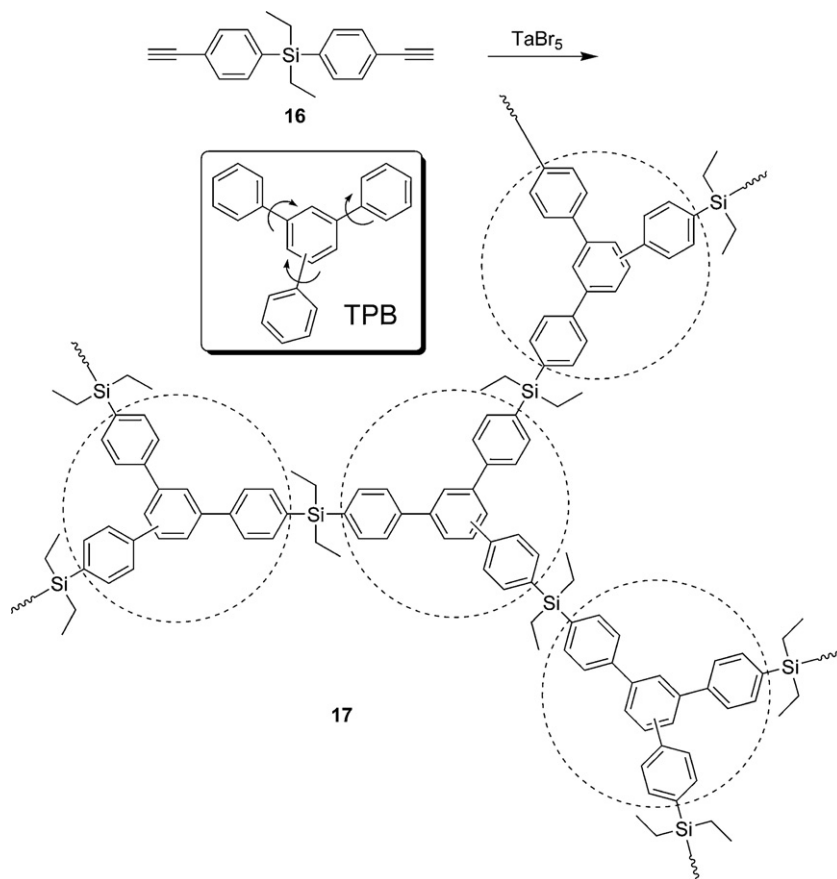© 2010, American Chemical Society.

Fig. 12. Synthesis of AEE-active σ^*–π^* conjugated hyperbranched poly(silylenephenylene) **17** by alkyne polycyclotrimerization. Inset: the composing unit of triphenylbenzene (TPB) [108].
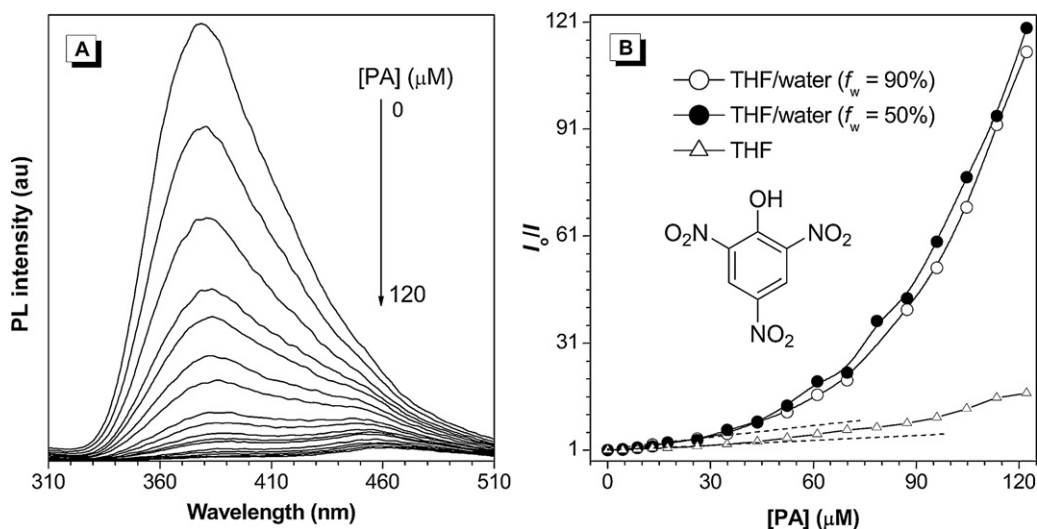
Fig. 13. (A) PL spectra of **17** in THF/water mixtures (f_w = 90%) with different amounts of PA. (B) Plot of I_0/I value versus PA concentration in THF and THF/water mixtures (f_w = 50 and 90%).
Reprinted with permission from Ref. [109].
© 2010, The Royal Society of Chemistry.

Encouraged by its AEE characteristic, **17** was applied as chemosensor to detect electron-deficient compounds such as nitroaromatic explosives in solution and aggregated states. The PL of **17** is weakened when picric acid (PA) is added into its THF solution or nanoaggregates in aqueous mixtures. The higher the PA concentration, the weaker is the light emission. Fig. 13A displays the PL quenching behavior of its nanoaggregates in the THF/water mixture with f_w = 90%. The PL quenching can be clearly discerned at a PA concentration as low as 1 ppm. The Stern–Volmer plot of the inverse relative PL intensity (I_0/I) versus PA concentration gives a curve bending upward, instead of a linear line. A similar curve is recorded in its nanoaggregates suspended in the aqueous mixture with 50% water fraction. The emission quenching observed in the aggregated state is much higher than that in the THF solution, manifesting a theoretically and practically important superamplification effect (Fig. 13B).

The possible reason for **17** to exhibit superamplification effect and give nonlinear Stern–Volmer plots is that it possesses a 3D topological structure with a relatively rigid aromatic scaffold, which contains many molecular cavities to capture small PA molecules through electrostatic or charge-transfer interactions (Fig. 14). Furthermore, thanks to the loose packing of the polymer branches and the additional diffusion pathways, the polymer nanoaggregates offer more cavities for the PA molecules to enter and interact with the chromophores, endowing the nanoaggregates of **17** with a higher sensitivity than their isolated species in solution.

Such a superamplification effect was also observed in AIE-active hyperbranched poly(silylenevinylene) **18**, which was synthesized by Rh-catalyzed alkyne polyhydrosilylation of 1,2-bis(4-ethynylphenyl)-1,2-diphenylethene with tris(4-dimethylsilylphenyl)amine in a high yield with a high molecular weight (Fig. 15) [111],
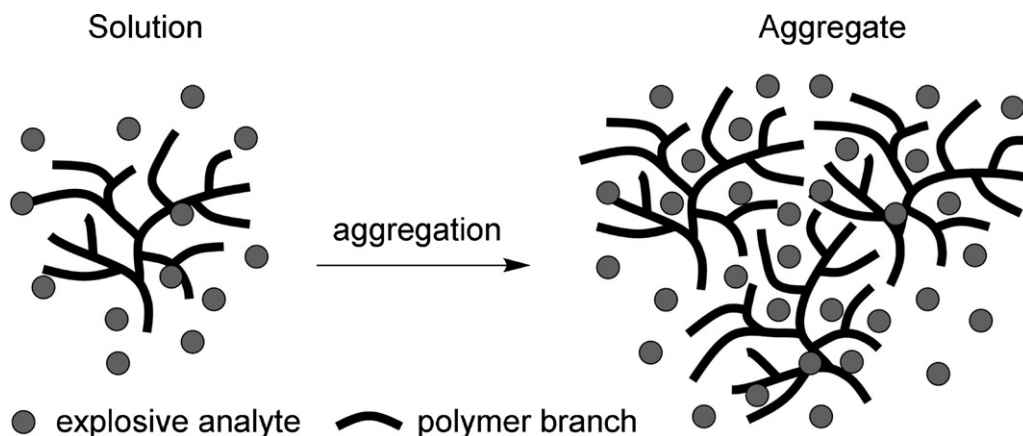

Fig. 14. Schematic illustration of detection of picric acid by AEE-active hyperbranched poly(silylenephenylene) **17** in solution and aggregate states.
Reprinted with permission from Ref. [109].
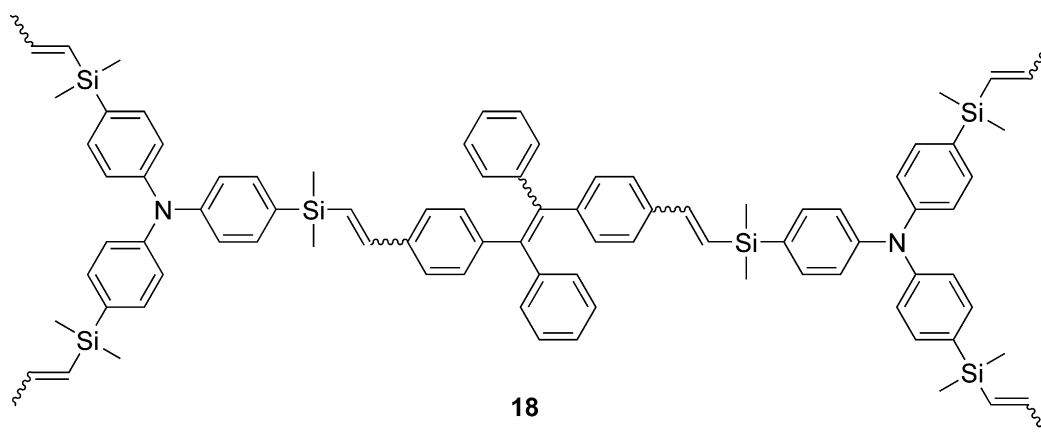© 2010, The Royal Society of Chemistry.

Fig. 15. Molecular structure of AIE-active hyperbranched poly(silylenevinylene) **18** [111].

manifesting that it is a general phenomenon observed in AIE/AEE-active polymers.

4. Polytriazoles

Since the first report in 2002, much attention has been placed on the copper-catalyzed azide-alkyne cycloaddition [112,113]. This reaction is so powerful that it has been referred to as "click chemistry" and hailed for its features which exhibit a number of remarkable advantages, including high efficiency, regioselectivity, atom economy, and tolerance to functional groups, and has found widespread applications in a great diversity of areas [114,115]. The utility of the click reaction in the area of polymer research has also been explored. While extensive studies have been done on the modification and functionalization of preformed polymers [116–118], effort has also been

devoted to foster the click reaction into a new polymerization technique [119,120].

Tang and co-workers utilized click polymerization in the syntheses of polytriazoles [121,122] as a natural extension of their research based on triple-bond building blocks. They introduced TPE unit to the polytriazole structure, which offers polymers (**22** and **23**) with AIE features [123]. Under optimized reaction conditions, **22** and **23** with high molecular weights were synthesized in high yields by click polymerizations of diyne (**19**) with diazides (**20** and **21**, Fig. 16) in THF using organo-soluble $Cu(PPh_3)_3Br$ as catalyst.

One problem for copper-mediated click polymerization is that the catalyst residue is difficult to remove completely from the polymeric product. The metallic residue can make the polymer insoluble during purification and storage because it may promote further polymerization in bulk or serve as cross-linker. It is also detrimental to the
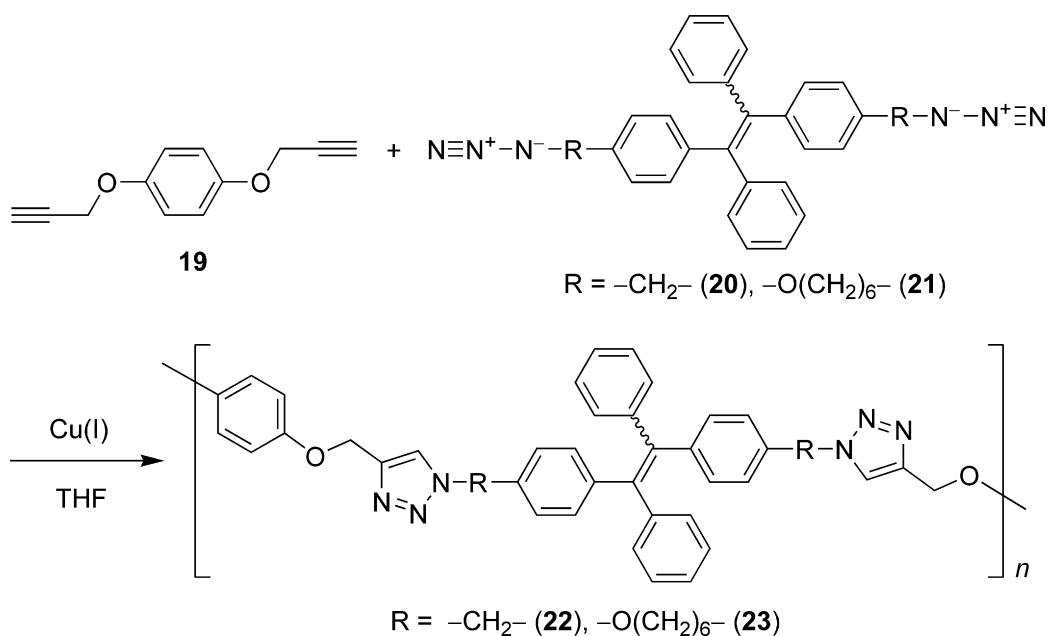

Fig. 16. Synthetic route to polytriazoles **22** and **23** by Cu(I)-catalyzed click polymerizations of diyne **19** with diazides **20** and **21** [123].
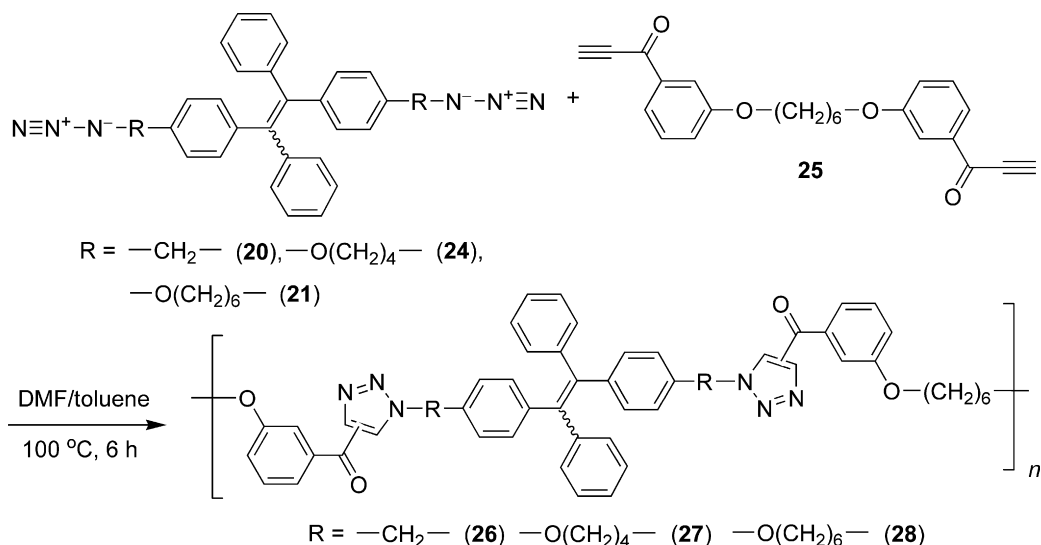
Fig. 17. Syntheses of TPE-containing PATAs **26–28** by metal-free click polymerizations [125].

electronic and optical properties of the synthesized polymers [124]. The development of non-metallic or metal-free polymerizations is thus highly desirable. For a metal-free system to be qualified as click polymerization, it must meet the definitions such as high regio-selectivity, good isolated yield, and mild reaction conditions. Furthermore, the polymerization reaction should be fast and the obtained products should be readily soluble.

Tang and co-workers found that aroylacetylene undergoes cycloaddition readily with azide under heating, generating regioregular aroyltriazole in high yield [122]. This fulfills the requirements for a click reaction and can be developed into a protocol for polymer preparation. Based on the above finding, they succeeded in synthesizing TPE-containing poly(aroyltriazole)s (PATAs) (**26–28**, Fig. 17) with high molecular weights (up to 25,200) and high

regioregularities (fraction of 1,4-isomer up to 95%) in high yields (up to 85%) and short reaction time from diazides (**20**, **21**, and **24**) and bis(aroylacetylene) **25** under optimized reaction conditions [125]. The polymers obtained are completely soluble in commonly used organic solvents, such as THF, chloroform, and dichloromethane (DCM).

Thanks to the incorporation of TPE moieties, all the poly(aroyl)triazoles **22**, **23**, and **26–28** are AIE-active. Fig. 18A shows the PL spectra of **23** in THF/water mixtures with different water fractions as an example; **23** is virtually non-luminescent when molecularly dissolved in dry THF. At f_w >50%, intense emission is recorded under identical measurement conditions in THF/water mixtures due to the aggregate formation.

The changes in the Φ_F values of the polymers with the water fractions in the aqueous mixtures further verify their
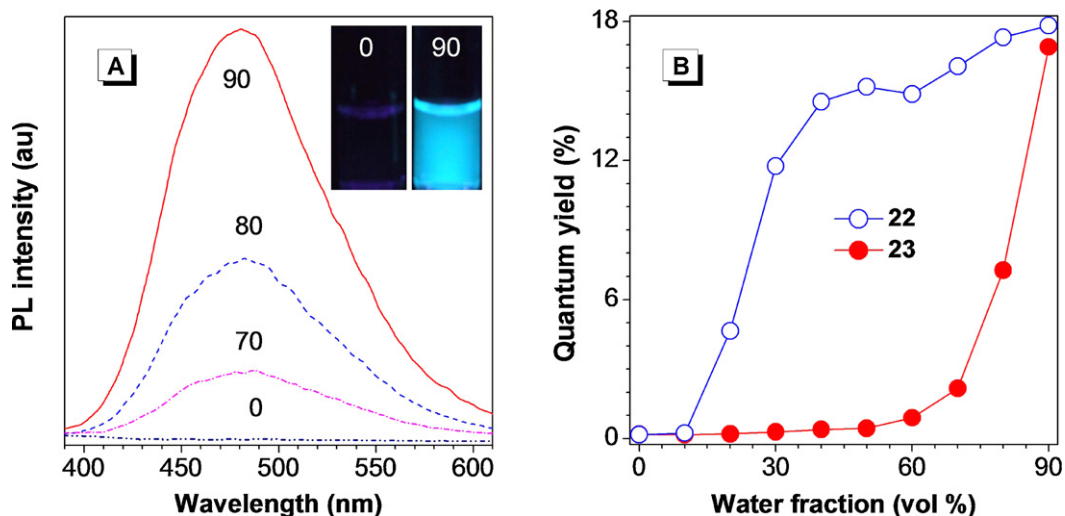

Fig. 18. (A) PL spectra of **23** in THF/water mixtures with different water fractions. (B) Variations in the quantum yields of **22** and **23** with water fractions in the aqueous mixtures (DMF/water for **22**; THF/water for **23**).
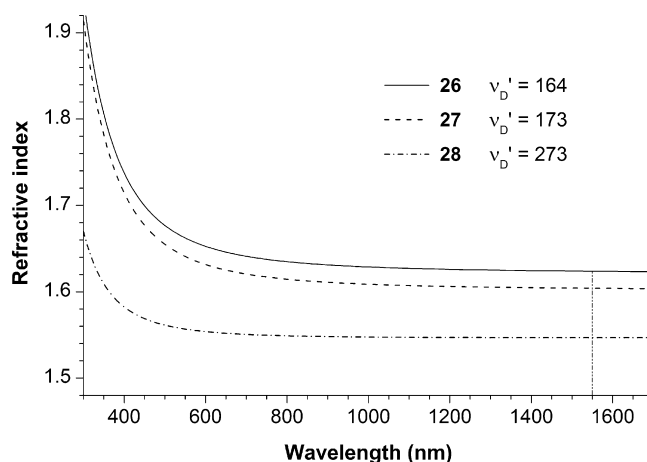Reprinted with permission from Ref. [123].
© 2009, American Chemical Society.

Fig. 19. Light refraction spectra of thin solid films of PATAs **26**–**28** and variation of modified Abbé numbers (ν_D') with polymer structures. Reprinted with permission from Ref. [125].
© 2009, Wiley-VCH Verlag GmbH & Co. KGaA, Weinheim.

AIE attributes. Both **22** and **23** exhibit negligibly small Φ_F values (0.16–0.18%) in THF (Fig. 18B). The Φ_F value of **23** remains almost unchanged at $f_W < 50\%$, while that of **22** begins to rise at lower water fractions ($\geq 10\%$) due to its lower solubility in aqueous medium. The Φ_F values of **22** and **23** at 90% aqueous mixtures are 17.8 and 16.9%, which are 110- and 94-fold higher than those in the THF solutions, respectively.

Furthermore, PATAs **26**–**28** are optically transparent in the whole visible spectral region and exhibit high and tunable refractive indices (RI) with high modified Abbé numbers (ν_D') owing to their partially conjugated structures and the presence of polarizable benzoyltriazole units. Wavelength-dependent RI measurement reveals that **26** possesses high RI values of 1.653–1.623 in the wavelength region of 600–1700 nm (Fig. 19). In the same wavelength region, its congeners with longer alkyl spacers, i.e. **27** and **28**, display lower refractive indices but their values are still higher than some commercial plastics. The difference in the RI value between **26** and **28** at the telecommunications important wavelength of 1550 nm is as large as 0.077. Thus, the PATAs may find high-tech applications as coating materials in the advanced display systems such as microlens components for charge-coupled devices and high-performance CMOS image sensors.

The AIE feature was also realized in polytriazoles with hyperbranched structures. Hyperbranched polytriazoles **31** containing TPE moieties were synthesized in high yields (up to 88.3%) by Cu(PPh$_3$)$_3$Br-catalyzed click polymerizations of triazides (**29**) and diyne (**30**) in DMF at 60 °C for 5–7 h (Fig. 20) [126]. Compared to the aforementioned AEE-active hyperbranched polyphenylenes, **31** possesses flexible spacers in its branches, which are responsible for its AIE effect. Polymers **31** are soluble in common organic solvents, such as THF, chloroform, and DCM. Analysis of **31** by size exclusion chromatography (SEC) relative to linear polystyrene standards gave apparent weight-average molecular weights up to 12,400; this procedure generally underestimates the molecular weight of hyperbranched architectures [127,128].

The hyperbranched polytriazoles are AIE-active. They are nonemissive in THF, but are induced to emit intensely by aggregate formation. An example of the PL spectra of **31a** in the aqueous mixtures is shown in Fig. 21A. Addition of water into the THF solution of **31a** has aggregated its chains and enhanced its light emission. The higher the water fraction, the stronger is the light emission. The Φ_F value also becomes higher with increasing water content in the THF/water mixture. At 90% aqueous mixture, the Φ_F values of **31a** and **31b** rise to 38.31 and 32.25%, which are 348.3 and 230.4-fold higher than those in pure THF solutions, respectively (Fig. 21B). The TPE luminogens are knitted inside the polymers via flexible spacers, which provide little constraint for the periphery phenyl rings to rotate in solution. In the aggregate state, the conformations of the polymers are tightly compressed due to the hydrophobic effects of the spacers and TPE units. This restricts the intramolecular motions of the polymers, which blocks the nonradiative path and activates the radiative decay, thus converting them from weak fluorophores to strong emitters. Such a result helps guide future molecular engineering endeavors in designing hyperbranched polymers with AIE characteristics.

5. Poly(phenyleneethynylene)s

To expand the variety of AIE-active polymers, Tang and co-workers recently prepared conjugated poly(phenyleneethynylene) containing TPE or silole units [129,130]. The inset in Fig. 22 shows an example of such polymer (**32**), which was synthesized by the Sonogashira coupling of 1,2-bis(4-iodophenyl)-1,2-diphenylethene with 1,2-bis(4-ethynylphenyl)-1,2-diphenylethene. Polymer **32** is soluble in common organic solvents, such as THF, chloroform, and DCM. It is somewhat emissive in THF and its emission intensity is enhanced by aggregate formation, showing a typical AEE phenomenon.

The AIE phenomenon has been reported in poly(phenyleneethynylene)s containing *o*-carborane units [131,132]. Carboranes are icosahedral clusters consisting
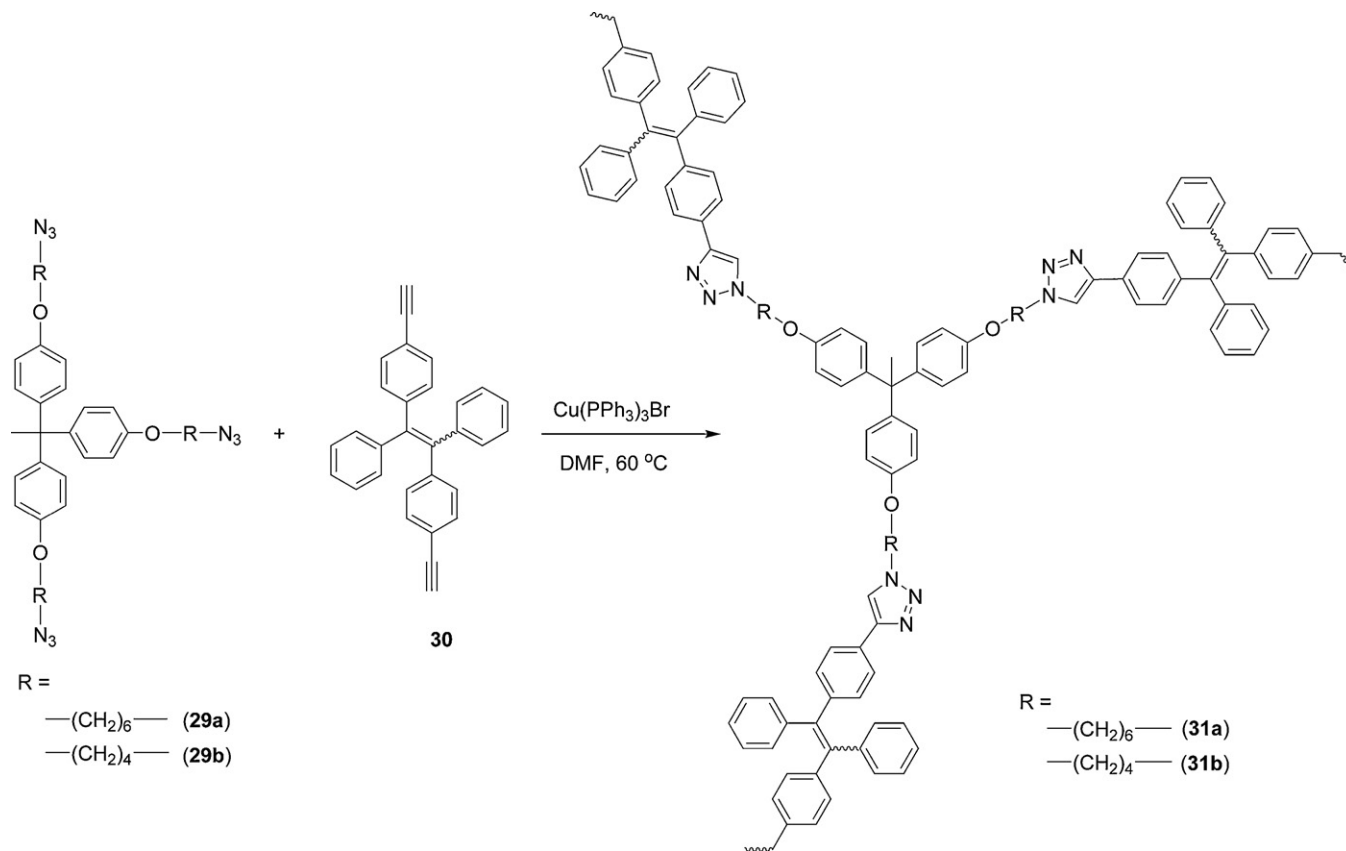
Fig. 20. Synthetic routes to AIE-active hyperbranched polytriazoles **31** by click polymerizations of **29** with **30** catalyzed by Cu(PPh$_3$)$_3$Br [126].
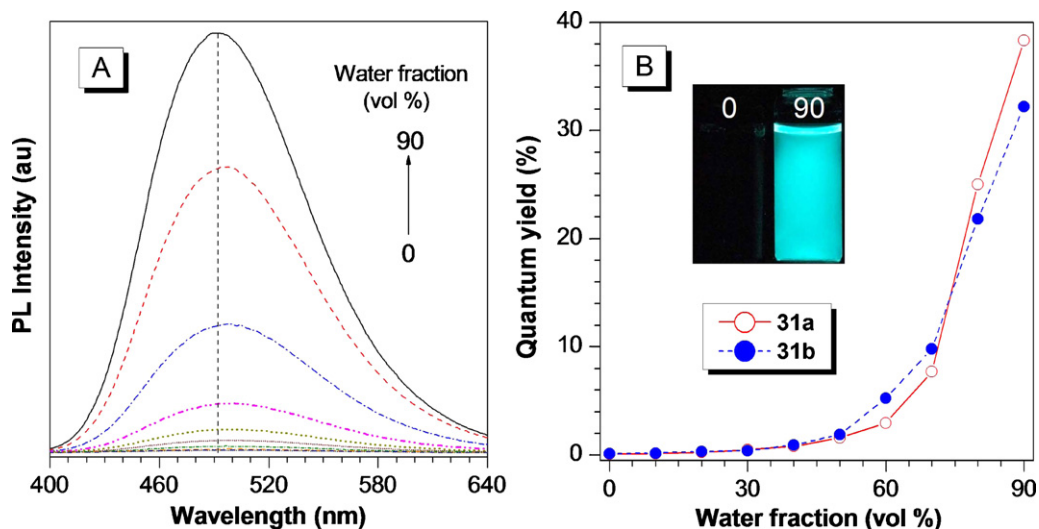
Fig. 21. (A) PL spectra of AIE-active hyperbranched polytriazole **31a** in THF/water mixtures with different water fractions, see panel (B). (B) Variation in quantum yields of **31a** and **31b** with water contents in THF/water mixtures. Inset in (B): photographs of **31a** in THF/water mixtures with 0 and 90% water fractions taken under UV illumination.
Reprinted with permission from Ref. [126].
© 2011, The Royal Society of Chemistry.

of 10 boron and 2 carbon atoms with three-center two-electron bonds and exhibit excellent thermal stability due to their three-dimensional aromaticity. Chujo and co-workers synthesized polymers **35** with moderate molecular weights in high yields from *o*-carborane derivative **33** and electron-donating diynes **34** by Sonogashira–Hagihara coupling polycondensation (Fig. 23). The degrees of polymerization for **35** are 3.5–7.6, which are lower than those in general poly(phenyleneethynylene)s [133], probably due to the steric effect of the *o*-carborane unit.

Polymers **35** are nonemissive in THF due to the intramolecular motions of the phenyl rings and charge transfer from the electron-donating *p*-phenyleneethynylene unit to

Fig. 22. Plot of PL intensity versus water fraction in the THF/water mixture of **32**. Inset: structure of **32**.

the anti-bonding orbital of the C–C bond in the *o*-carborane cluster [132]. In the THF/water mixture with 99% water fraction or in the film state, **35** displays bright orange light owing to the restriction of tortional/vibrational motions and charge transfer between the alternating donor and acceptor segments in the polymer backbone [131].

Measurements of the Φ_F values of the polymers in the THF/water mixtures with different water fractions provide additional insights into their AIE phenomena. Polymers **35a** and **35b** are taken as examples (Fig. 24). The Φ_F values of the polymers are negligible (<0.02%) in THF and remain unchanged when up to 50% of water is added to their THF solutions. Afterwards, the values rise swiftly. The Φ_F value of **35a** at $f_w = 99\%$ reaches 3.8%, being 220-fold higher than that in THF. These results indicate that the introduction of luminescent π-conjugated segments into the 1,2-positions of the *o*-carborane units in poly(phenyleneethynylene)s has endowed the resultant polymers with AIE characteristics.

6. Poly(phenylenevinylene)s

Tang and co-workers investigated the synthesis of conjugated poly(phenylenevinylene)s bearing TPE luminogens (Fig. 25) [129,130]. Polymers **36** and **37** possess moderate molecular weights (4,400 and 11,800, respectively) and are soluble in common organic solvents.

Fig. 26 shows the photographs of **37** in THF/water mixtures; **37** emits green light in THF albeit in low efficiency. Gradual addition of water into its THF solution has, however, progressively intensified its emission; in other words, **37** is AEE-active.

More importantly, **37** exhibits an aggregation-enhanced two-photon excited fluorescence (AETPEF) effect. As shown in Fig. 27, the two-photon excited fluorescence (TPEF)

Fig. 23. Preparation of AIE-active polymers **35** bearing *o*-carborane units [131,132].

Fig. 24. Variation in the quantum yields of **35a** and **35b** with water fractions in THF/water mixtures.
Reprinted with permission from Ref. [131].
© 2009, American Chemical Society.

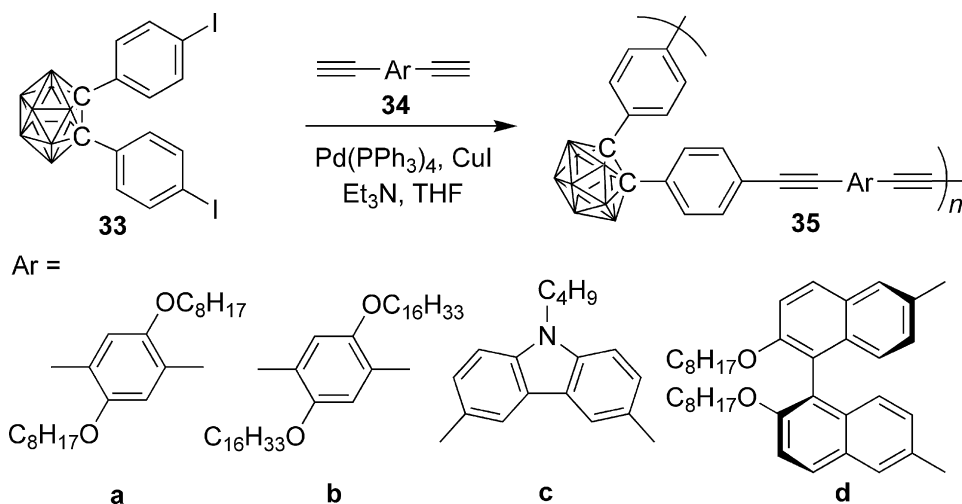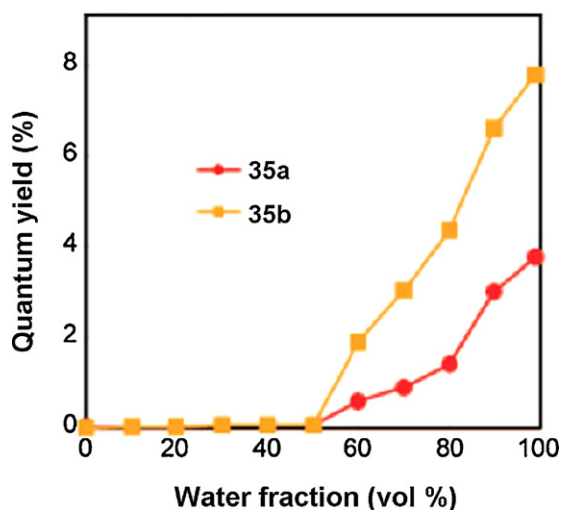intensity of its nanoaggregate is ∼9-fold higher than its isolated chain in the THF solution when excited at 800 nm with a femtosecond laser pulse. The profile of the one- and two-photon excited fluorescence spectrum is similar, manifesting that they are originated from the same radiative species. The two-photon absorption cross-sections of **37** in the solution and aggregated states are measured at 750 nm to be 107 and 896 GM, respectively, which are comparable to many reported organic molecules. Since the two-photon technique allows intact tissue imaging due to its advantages of increased penetration depth, localized low energy excitation, and prolonged observation time, **37** is a promising light-emitting material for biological applications [134,135].

7. Poly(thienylazulene)s

The azulene-containing conjugated polymers have been widely investigated because azulene possesses non-alternating aromatic structure and unusual physical properties, as well as anomalous fluorescence from the second excited state to the ground state [136]. A team led by Han and Lai reported that poly{1,3-bis[2-(3-alkylthienyl)] azulene} and poly{1,3-bis[2-(3-alkoxythienyl)]azulene}
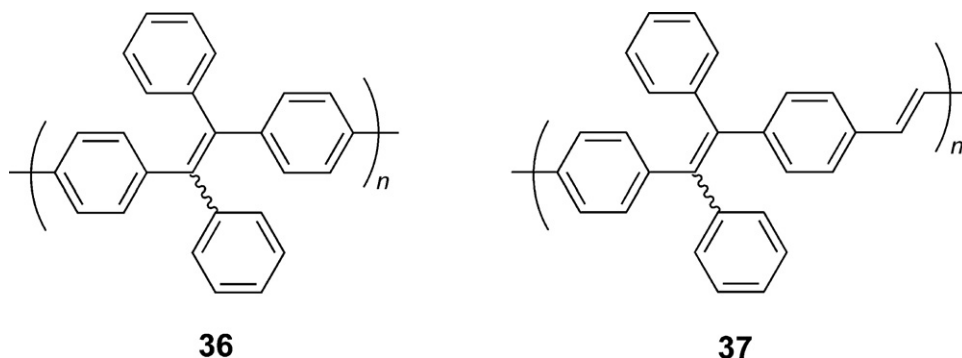

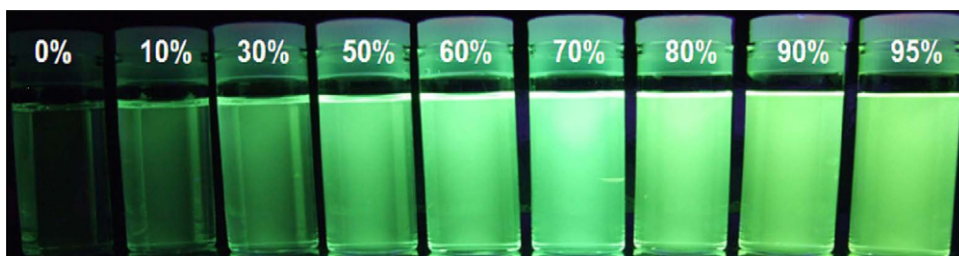**Fig. 25.** Molecular structures of TPE-containing polymers **36** and **37**.

Fig. 26. Fluorescent photographs of **37** in THF/water mixtures with different water fractions taken under UV illumination.

with ~40–50 repeat units can form size-tunable nanoparticles through chain aggregation [137]. The nanoparticles were prepared by vigorously mixing the polymers in chloroform/methanol mixtures (f_m = 50%) at an optimized concentration of 20 μM. The time-dependent size evolutions of the nanoparticles were followed by dynamic light scattering and field-emission scanning electron microscope (SEM). Fig. 28 depicts the SEM images of the nanoparticles of alkyl-substituted poly(thienylazulene) **38**, whose molecular structure is given in the inset of Fig. 29A, as an example. In the first minute, the particle grows to ~60 nm in diameter, increasing to 120, 240, and 400 nm when time elapses from 10, 60, to 240 min, respectively.

The polymers are nonemissive in chloroform, but become luminescent when aggregated. The PL behavior of **38** is demonstrated in Fig. 29A. The emission of the polymer is enhanced gradually with increasing particle size in chloroform/methanol mixture (f_m = 50%) with time. The linear dependence of the PL intensity on the particle size demonstrates that the polymer possesses unique size-dependence emission properties (Fig. 29B), which can be used as a sensitive probe to study the intermolecular interactions and the size evolution of conjugated polymer
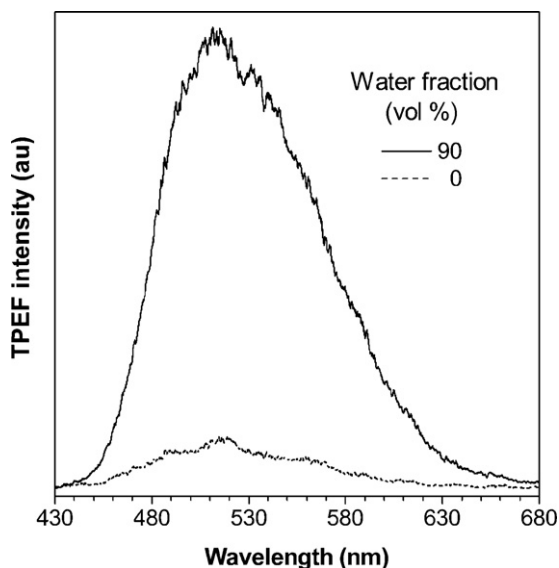
nanoparticles, although the reason for such a relationship remains unclear at present. The nonemissive nature of **38** in chloroform is attributed to the active intramolecular rotation of the thiophene rings around the axes of the single bonds linked to the azulene rings, which serves as a relaxation channel for the excited state to decay. When **38** forms nanoparticles, the torsional rotations between the thiophene moieties and the central azulene rings are restricted, which makes the polymer highly emissive.

8. Polysilole

Since siloles are AIE-active [138], their polymers with linear and hyperbranched structures are also anticipated to show similar emission behaviors. Sohn and co-workers had synthesized polysilole **40** with a moderate molecular weight by reduction of 1,1-dichlorotetraphenylsilole (**39**) with lithium in THF (Fig. 30) [139–141].

Polysilole **40** is weakly emissive at ~520 nm when molecularly dissolved in THF (Fig. 31). The PL intensity remains almost unchanged when less than 40% water is added to the THF solution. Afterwards, it rises swiftly without any shift in the peak maximum, revealing that the aggregate formation has little impact on the molecular configuration. The highest PL intensity was recorded in the THF/water mixture at f_w = 99%, which is ~18-fold higher than that in THF. The plot of PL intensity versus water fraction in the aqueous mixture gives an exponential upward curve, further confirming that **40** is indeed AEE-active.

9. Polyolefins

The polymers discussed in the previous sections possess conjugated structures. In this section, we consider electronically saturated polymers such as polyolefins featured with AIE/AEE characteristics.

Chi and Xu designed and synthesized a group of carbazole-substituted triphenylethenes and found that they are AIE-active with strong blue light emission and high thermal stability [142]. Recently, they succeeded in preparing a polystyrene **42** containing one of these luminogens in a high yield with a high molecular weight and good solubility by AIBN-initiated radical polymerization of **41** (Fig. 32) [143].

Different from its AIE-active monomer **41**, **42** is emissive in THF (Fig. 33). Addition of water into its THF solution has aggregated its chains and enhanced its light emission. In 90% aqueous mixture, the PL intensity is 8-fold higher than that in THF, demonstrating AEE behavior. With this

Fig. 27. TPEF spectra of **37** in THF/water mixtures with 0 and 90% water fraction measured under femtosecond excitation at 800 nm. Concentration: 2.6 μM.
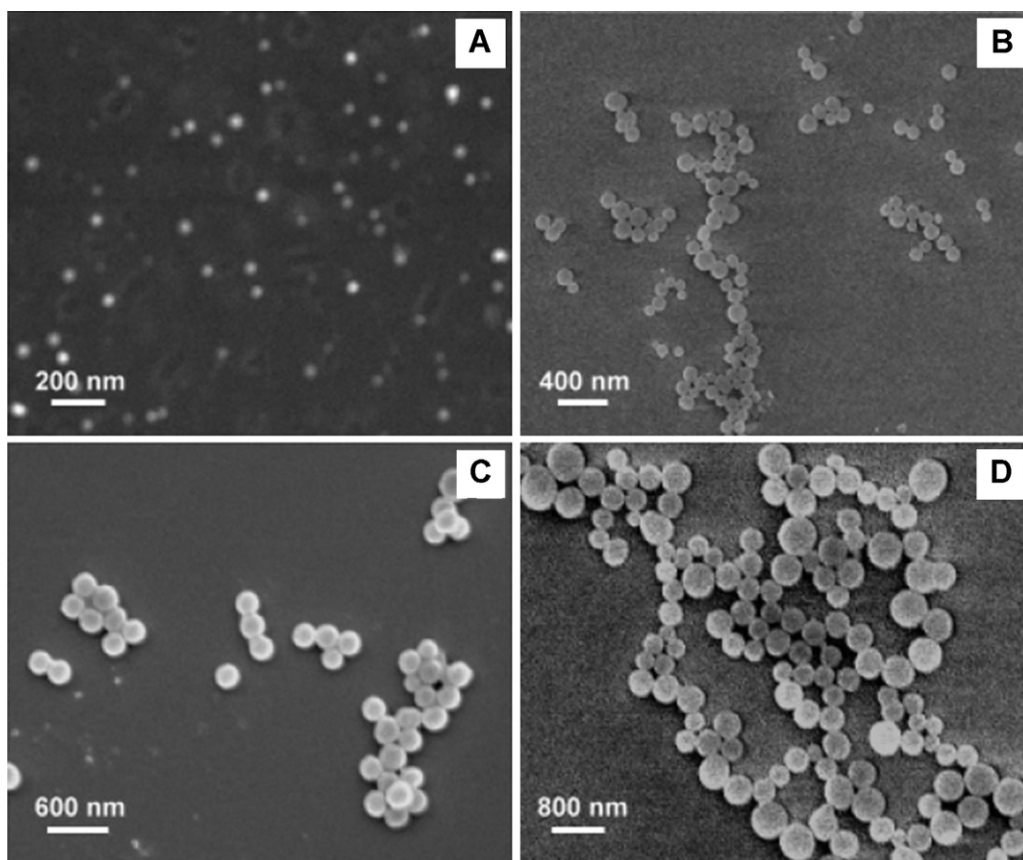
Fig. 28. SEM images of nanoparticles of **38** formed in chloroform/methanol mixture with 50% methanol fraction at (A) 1 min, (B) 10 min, (C) 60 min, and (D) 240 min.
Reprinted with permission from Ref. [137].
© 2005, American Chemical Society.
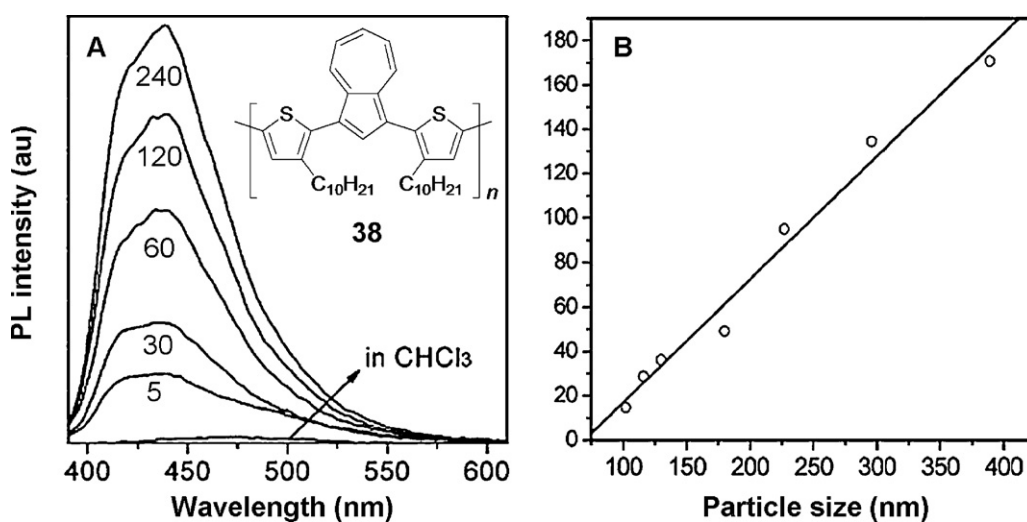
Fig. 29. (A) PL spectra of nanoparticles of **38** formed in chloroform/methanol mixtures with 50% methanol fraction at different time intervals (unit: min). Inset: polymer structure of **38**. (B) Dependence of the PL intensity on the size of nanoparticles of **38**.
Reprinted with permission from Ref. [137].
© 2005, American Chemical Society.
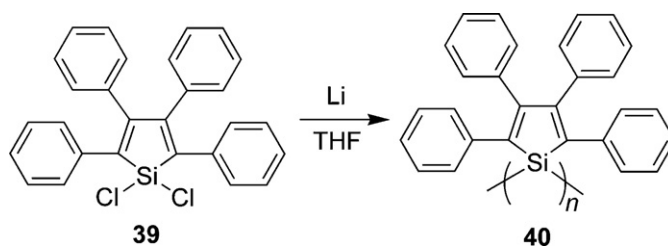
Fig. 30. Synthetic route to polysilole **40** [140].
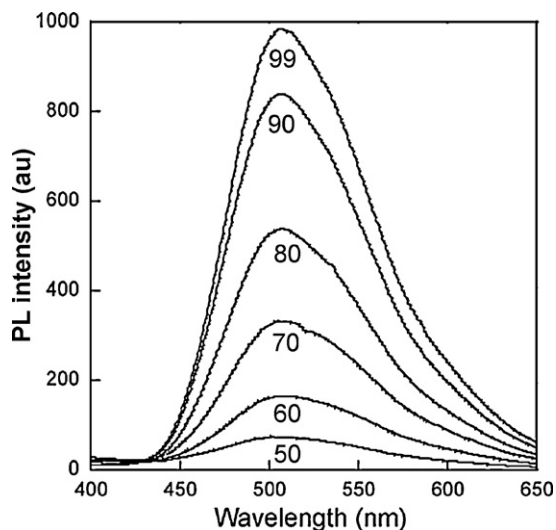
Fig. 31. PL spectra of polysilole **40** in THF/water mixtures with different water fractions.
Reprinted with permission from Ref. [139].
© 2006, The Korean Chemical Society.
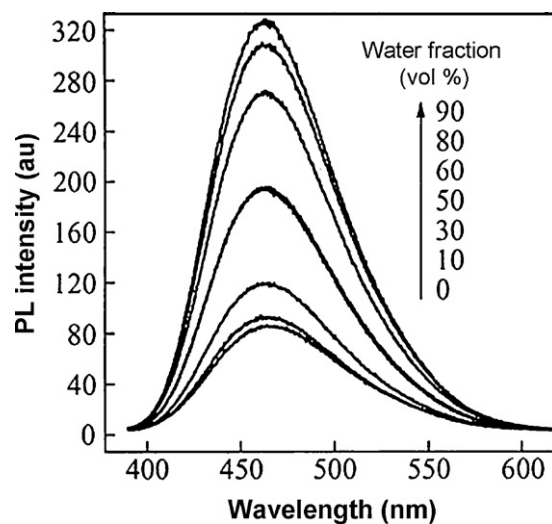
Fig. 33. PL spectra of polystyrene **42** in THF/water mixtures with different water fractions.
Reprinted with permission from Ref. [141].
© 2009, Acta Polymerica Sinica.

feature, **42** can be considered for a potential vapor sensor for volatile solvents such as DCM.

Hong and co-workers reported the AEE phenomenon of quinoline-containing poly(vinyl 2,4-enylquinoline) (**43**), as well as its complex with camphorsulfonic acid (CSA) (**44**) (Fig. 34) [144]; **43** was prepared by Friedländer condensation of 2-aminobenzophenone and poly(4-acetyl styrene), and complex **44** was obtained by stirring a mixture of equivalent molar of **43** and CSA in chloroform for 24 h.
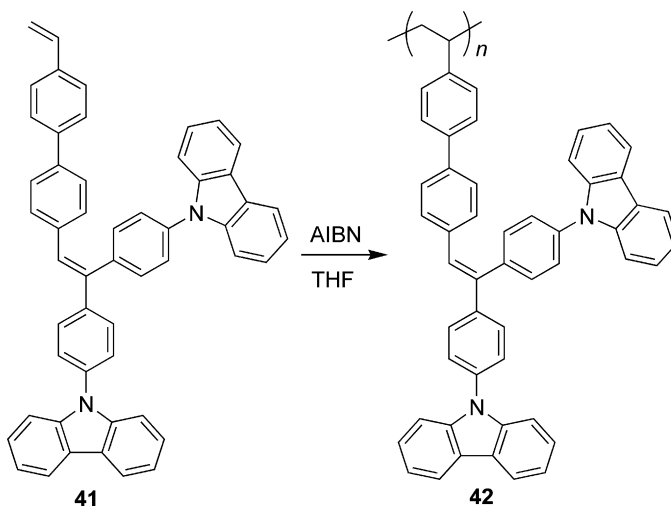
Fig. 32. Synthetic route to AEE-active polystyrene **42** [143].

Table 1
Φ_F values of **43** and **44** measured from the solution mixtures and the solid samples.[a]

	$f (\%)$						
	0	30	60	70	80	90	Solid
From dilute solutions (10^{-4} M) of **43** in THF/water mixtures							
43	0.021	0.032	0.033	0.034	0.036	0.037	0.043
From dilute solutions (10^{-4} M) of **44** in THF/hexane mixtures							
44	0.116	0.185	0.283	0.336	0.378	0.381	0.667

Reprinted with permission from Ref. [144].

[a] f: water or hexane fraction in THF/water or THF/hexane mixtures.
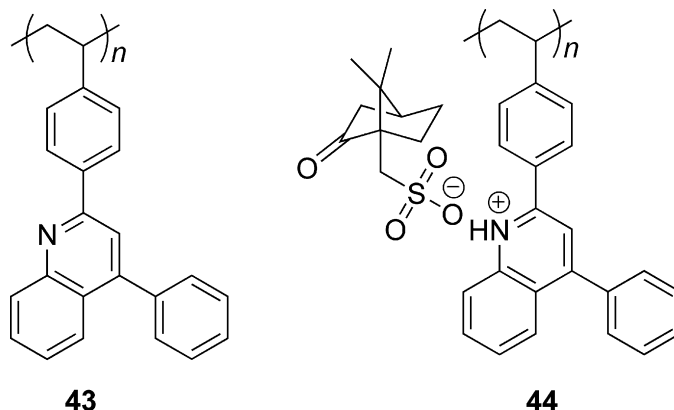
Fig. 34. Chemical structures of quinoline-containing polymer **43** and its complex with camphorsulfonic acid (**44**) [142].

The AEE effect of **43** and **44** was demonstrated by addition of poor solvents into their THF solutions. Measurement on their Φ_F values further verified their AEE characteristics (Table 1). Their Φ_F values become higher with increasing water fraction in the THF/water mixture and reach their maximum in the solid state. The Φ_F value of **44** is much higher than **43** because the bulky CAS moiety has partially hindered the rotation of the phenyl rings of the quinoline unit. Such work provides a strategy to further enhance the emission of luminogenic polymers with AIE/AEE effects in the condensed phase.

Tang and co-workers prepared TPE-containing cross-linked polyacrylates (**45**–**47**) with high molecular weights in nearly quantitative yields by radical polymerizations of their corresponding monomers (Fig. 35). All the polymers are soluble in common organic solvents, such as THF, and DCM, facilitating their structural characterization and property investigation by "wet" spectroscopic techniques.

Yield: 97 %
M_w: 87100

45

Yield: 99 %
M_w: 19600

46

Yield: 99 %
M_w: 33400

47
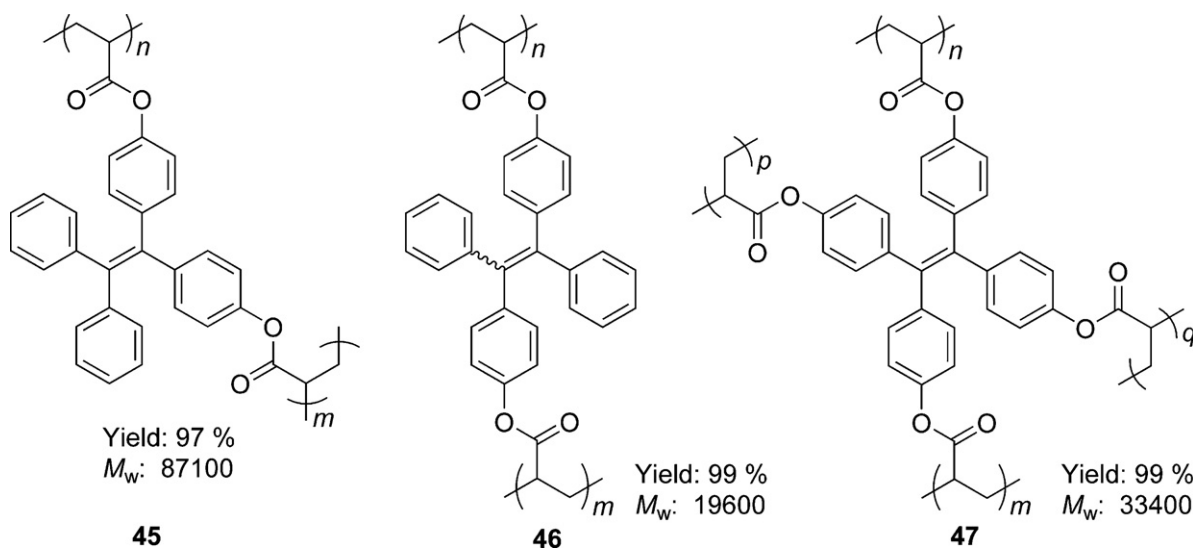
Fig. 35. Chemical structures of TPE-containing cross-linked polyacrylates **45**–**47**.
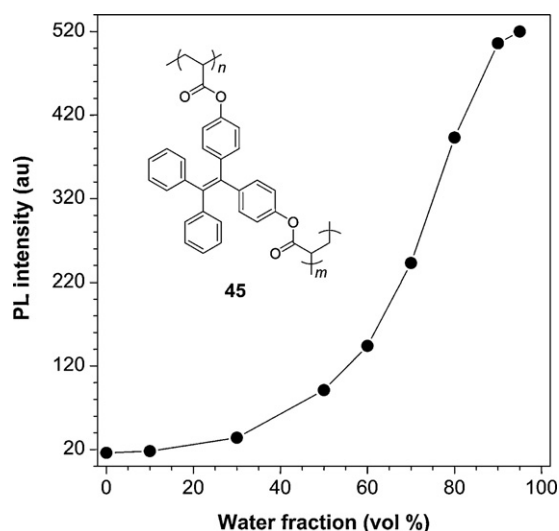
Fig. 36. Dependence of emission intensities of **45** on the water fractions in THF/water mixtures.

These cross-linked polyacrylates exhibit AEE features due to the partial restriction of the motions of the phenyl rings by the rigid polymer skeleton. Fig. 36 shows the change in the PL of **45** with the water fraction in the THF/water mixture as an example. In THF, **45** exhibits a weak emission at ∼460 nm. Addition of water into the THF solution enhanced the light emission by up to ∼32-fold.

Poly(*N*-isopropylacrylamide) (PNIPAM) has drawn much attention in recent years and has been widely investigated due to its interesting thermo-responsive property. Such polymer undergoes conformational transition from hydrated coil to dehydrated globule in water with lower critical solution temperature (LCST) at around 32 °C. Tang and co-workers labeled PNIPAM with TPE moiety to develop a fluorescent thermometer operated via a novel AIE mechanism under neutral conditions [145]. The TPE-functionalized alkene (**48**) was synthesized by copper-catalyzed click reaction and was radically copolymerized with NIPAM **49** to produce copolymer **50** (Fig. 37). The amount of incorporated TPE was adjusted in the range

of 0.27–1% to diminish its impact on the performance of PNIPAM. PNIPAM containing 0.27% TPE unit (**50a**) is taken as example for the following discussion.

50a is nonemissive in good solvents for both TPE and PNIPAM such as THF (Fig. 38). Its emission becomes visible when a large amount (≥70%) of water was added into its THF solution (Fig. 38C), indicating that the TPE label renders its AIE activity after being incorporated into the PNIPAM structure.

The temperature effect on the PL behavior of **50a** in water is shown in Fig. 39. The PL spectrum of the polymer exhibits little change when the solution is heated from 14 to 25 °C. A small bump appears in the temperature region of 25–29 °C. Afterwards, the emission intensity increases swiftly and reaches its maximum at a temperature of 34.2 °C. Further increment of the temperature, however, leads to a gradual decrease in the PL intensity. When the solution is cooled from 50 to 18 °C, the spectrum completely reappears within experimental error. This result shows that the fluorescence-based tool is more sensitive and informative than other analytical techniques that display a monotonic temperature-dependence.

When the temperature is lower than 25 °C, the polymer chain may be well dispersed; the hydrophobic TPE labels, however, may have been loosely wrapped by the polymer coils or aggregated into tiny particles, which partially restrict the motions of the phenyl rings and thus make the polymer luminescent in water. When the temperature reaches 25 °C, the polymer chains begin to dehydrate from the isopropyl pendants. This partially damages the water cages surrounding the polymer coils and promotes the dehydrated chain segments to undergo a coil-globule transition, which is sensitively visualized by the TPE label.

At the temperature region of 29–34 °C, not just the pendants and segments but also the whole polymer chains dehydrate, resulting in the formation of compact aggregates. This process greatly activates the RIR process of the TPE labels and thus makes the system highly emissive. Further heating the mixture to above 34 °C may cause the aggregates to grow bigger. Consequently, the TPE labels may have been encompassed and no UV excitation beam can be reached. Meanwhile, the elevated
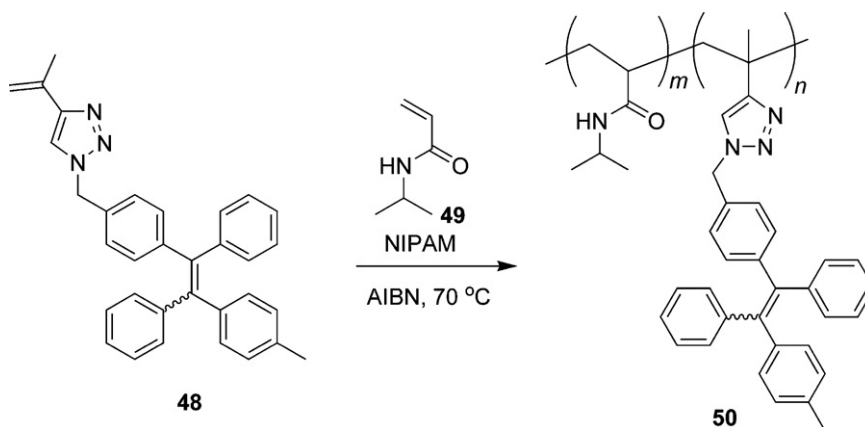
Fig. 37. Synthetic route to TPE-containing PNIPAM **50** [143].
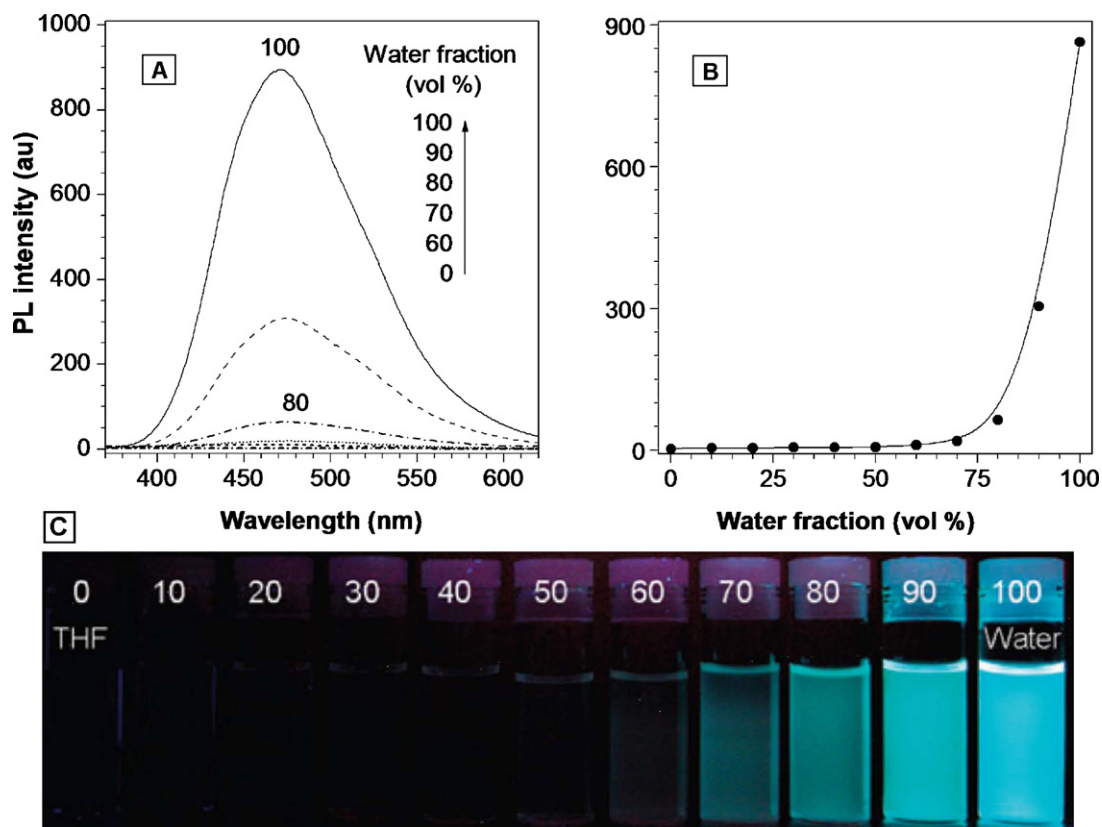
Fig. 38. (A) PL spectra of **50** in THF/water mixtures with different water fractions measured at 17 °C. (B) Variation in maximum emission intensity of **50** with water fraction in the THF/water mixture. (C) Photographs of THF/water mixtures of **50a** with different water fractions taken under UV illumination. Reprinted with permission from Ref. [143].
© 2009, The Royal Society of Chemistry.
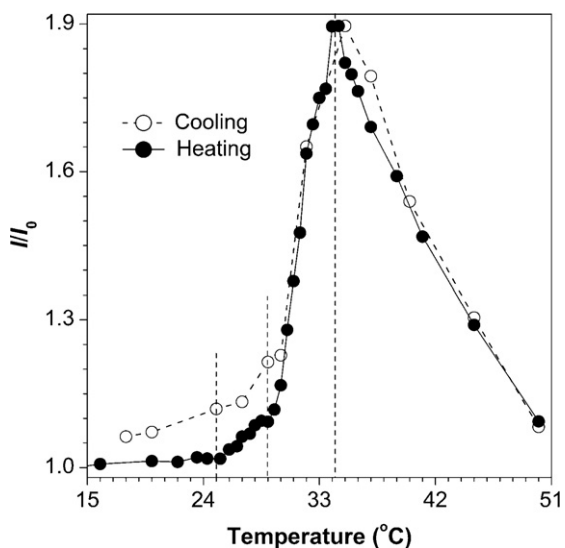
Fig. 39. Effect of temperature on the relative PL intensity (*I*) of **50a** at 468 nm.
Reprinted with permission from Ref. [143].
© 2009, The Royal Society of Chemistry.

temperature may activate the motions of the phenyl rings. These two effects collectively make the system less emissive. Although further investigation is needed, the present result demonstrates a promising tool for detecting tiny temperature change in biological system.

During the course of exploration of new AIE system, Tang and co-workers noticed an unusual AIE phenomenon in poly[(maleic anhydride)-*alt*-(vinyl acetate)] (**51**) in 2007, which possesses no chromophoric units [146]. Fairly uniform colloidal particles of **51** with tunable sizes can be obtained by the copolymerization of maleic anhydride and vinyl acetate in butyl acetate (Fig. 40) [147]. Whereas **51** emits faintly in THF, its suspended colloids in butyl acetate give blue light of ∼420 nm, whose intensity increases with increasing concentration. Since the copolymer is not conjugated, the RIR mechanism may not be applicable for such AEE phenomenon. It is speculated that the close packing of the anhydride carbonyl groups of the polymer plays a crucial role in its emission. More experiments and theoretical calculations need to be conducted to decipher its mechanism and help further development of new photophysical theory.

A similar phenomenon was also reported by Pucci and co-workers with maleic anhydride grafted polyisobutene
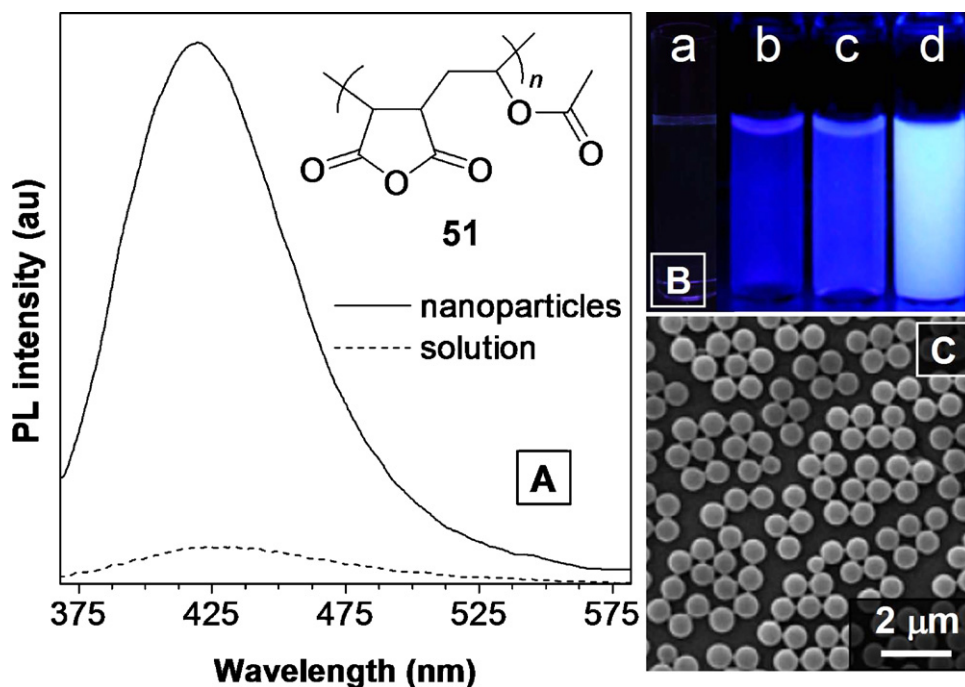
Fig. 40. (A) Emission spectra of nanoparticle suspension of **51** in *n*-butyl acetate and its solution in THF. Inset: polymer structure of **51**. (B) Fluorescent images of THF solution (a) and nanoparticle suspensions in *n*-butyl acetate with concentrations of (b) 0.05 wt%, (c) 0.1 wt%, and (d) 1 wt% taken under UV illumination. (C) SEM image of the nanoparticles [144].

in 2008 [148]. The thermal-induced radical end-capping reaction of the terminal vinyl unit of polyisobutene with large amount of maleic anhydride was stopped at time intervals of 4, 7, 10, and 14 h, generating polyisobutene succinic anhydrides (PIBSAs) **52–55** with different anhydride contents [149]. Interestingly, PIBSA obtained at 4 h shows a faint fluorescence in heptane (1.45 mM), but became more emissive when isolated at longer reaction times. The PIBSA collected after 10 h shows a reasonably high PL intensity in heptane due to its high degree of functionalization (>2) [150]. The emission of PIBSA generated at 7 h was also enhanced in hepane when the solution concentration was varied from 16.5 μM to 3.20 mM.

After exclusion of the emission from impurities or polyisobutene, Pucci and co-workers attributed this unusual PL behavior to the formation of aggregates from the succinic anhydride moieties grafted to the polyisobutene backbone (Fig. 41). The PIBSAs are molecularly dissolved in heptane in the early reaction stage of their formation, which makes them faintly emissive. Prolonging the reaction time increases the succinic anhydride content in PIBSAs, which enables such units to aggregate and interact strongly with the adjacent moiety in heptane. This may effectively reduce the nonradiative relaxation of the carbonyl groups, endowing the polymers with intense emission.

10. Poly(acylhydrazone)s

Dynamers are dynamic polymers and are synthesized by reversibly connecting monomers through covalent or non-covalent bonds [151]. Such polymers are capable of varying their constituent, length, and sequence, enabling modification of their mechanical and optical properties by changing the feed components during polymerization or by adding another monomer after polymerization. During the extension of their dynamer research to biopolymers, Lehn and co-workers found that the biodynamers with oligosaccharide residues are emissive but most of their monomers are nonluminescent [152,153].

The glycodynamer analogues of poly(acrylhydrazone)s were synthesized by polycondensation of dilute solutions of oligosaccharide-containing aromatic dialdehydes and bishydrazides in D_2O under mild acidic conditions (pD = 4–6). A representative synthetic route to **58** was shown in Fig. 42 as an example. The molecular weight of **58** was measured to be 511,000, corresponding to about 275 monomeric units.

Whereas most of the dialdehydes and bishydrazides are nonemissive in D_2O, the resultant glycodynamers are highly luminescent. This phenomenon likely originates from their tightly packed polymer structures, in which the aromatic hydrazone units are isolated and rigidly held in the hydrophobic core. This restricts their intramolecular rotations that serve as nonradiative channels for the excitons to relax. Depending on their monomer counterparts, the glycodynamers can emit strong light from blue to red. The emission color of a preformed dynamer can be changed by the addition of another monomer, illustrating the dynamic equilibrium nature of the glycodynamer constituent. These optodynamers are thus potentially useful as adaptive fluorescent probes and effective responsive optical materials.
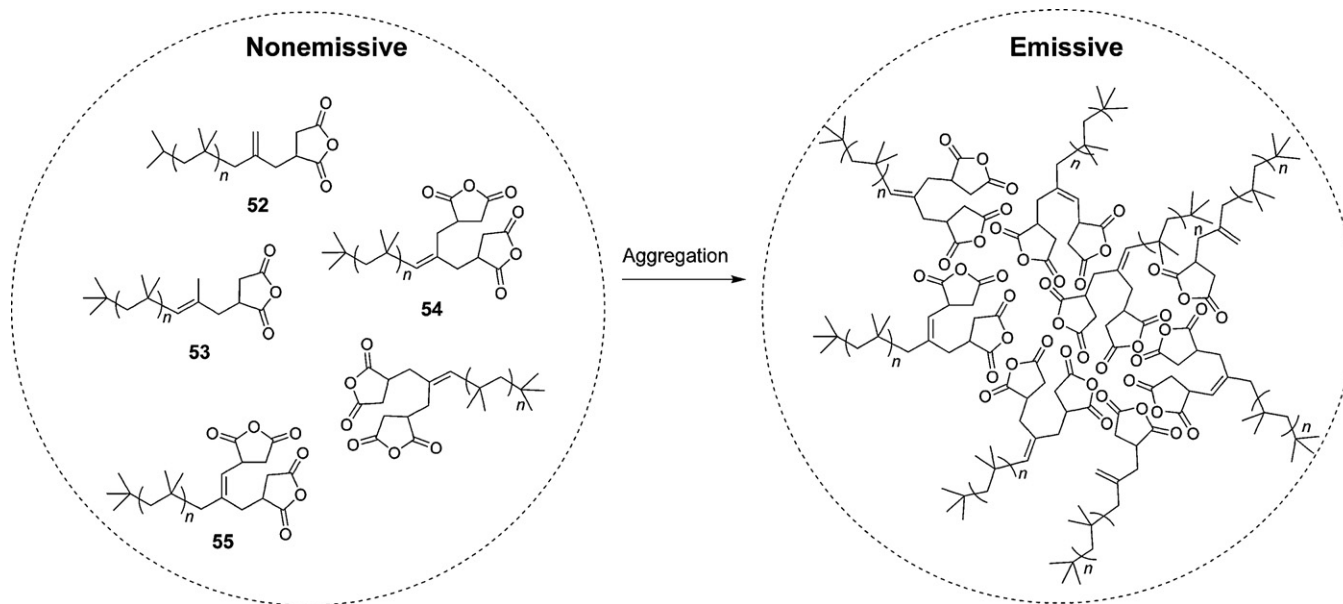
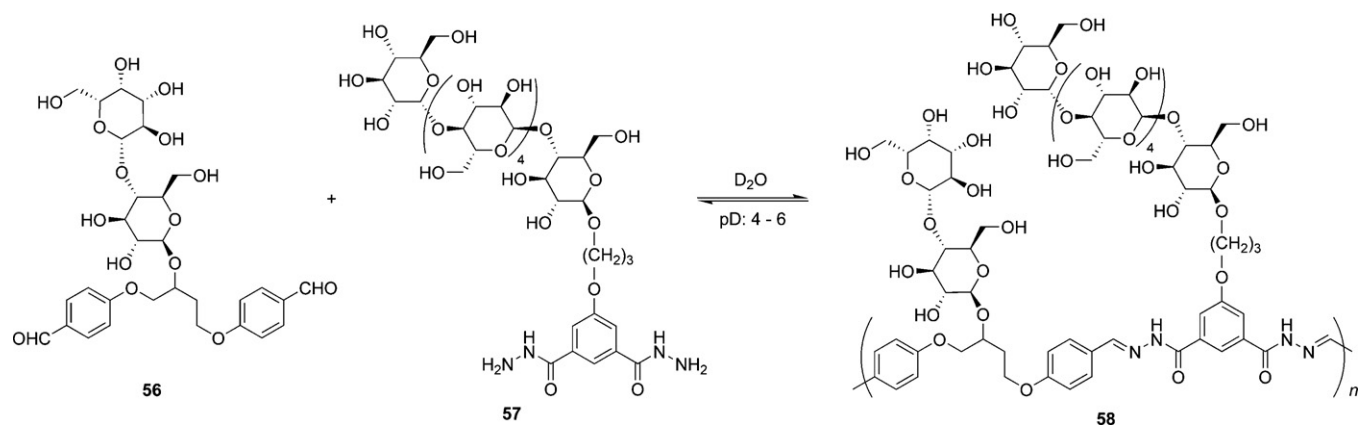**Fig. 41.** Schematic illustration of aggregation of PIBSAs **52**–**55** [148].

Fig. 42. Preparation of dynamic poly(acylhydrazone) **58** by polycondensation of **56** and **57** [150].

11. Conclusions and outlook

Recent research efforts on the design and synthesis of AIE/AEE-active luminogenic polymers with linear and hyperbranched structures are summarized in this review. The general strategy to synthesize such polymers is by attaching propeller-like AIE-active moieties, such as TPE and silole, as pendants to the polymer backbones or utilizing these units as building blocks for main-chain polymers. The change in the emission behavior from AIE characteristic in low-molecular-weight molecules to AEE feature in polymers especially with hyperbranched structures provides new evidence that restriction of intramolecular motion is the main origin of the AIE effect. An interesting AIE phenomenon has been observed in succinic anhydride-containing non-conjugated polymers without chromophoric units, probably owing to the agglomeration of carbonyl groups.

Some interesting AIE/AEE features can only be realized in polymeric systems. For example, maleic anhydrides are AIE-inactive either in the solution or in the solid state, but polyisobutenes decorated with these moieties exhibit AIE feature. Emission superquenching has been observed in polymers particularly with hyperbranched architectures due to their unique structures as well as morphologies in the aggregate state.

The AIE/AEE-active polymers exhibit an array of functional properties. Polymers bearing (meth)acrylate and benzoyltriazole units are highly photosensitive and can generate fluorescent photoresist patterns upon UV irradiation. The high polarizability of the triazole rings in poly(aroyltriazole)s has endowed them with high and tunable refractive indices. Novel and unique aggregation-enhanced two-photon excited fluorescence and large two-photon absorption cross-sections are realized in TPE-containing conjugated poly(phenylenevinylene)s in the aggregate state.

Although remarkable progress and exciting results have been achieved, research on AIE/AEE-active polymers is still in its infancy and many possibilities are still awaiting exploration. Opportunities will exist in enriching the variety of AIE/AEE polymers, investigating the mechanism, developing new functional properties, and exploring potential electro-optical and biological applications. Currently, most of the approaches on the construction of AIE/AEE-active polymers are based on the incorporation of AIE-active low-molecular-weight molecules into the macromolecular structures. Thus, development of polymers with in situ generated AIE/AEE features will be a promising direction. Further exploration of their potential applications, especially in light-emitting diodes, chemosensors, and bioprobes, will also be an exciting research topic. Understanding the working principle for the AIE phenomenon of polymers without luminogens will be a challenging and important work for further development of new AIE systems.

It is anticipated that by enthusiastic research efforts of scientists, a variety of AIE/AEE-active polymers with linear and hyperbranched structures will be generated, which exhibit versatile properties that are not observed in traditional conjugated polymers. It is hoped that this review may serve as a "catalyst" to stimulate new enthusiasm of scientists to be involved in this emerging and promising field, and to trigger new ideas and accelerate the pace in the design and synthesis of new AIE-active polymers with novel functionalities for high-tech innovations.

References

[1] Tang CW, VanSlyke SA. Organic electroluminescent diodes. Appl Phys Lett 1987;51:913–5.
[2] Burroughes JH, Bradley DDC, Brown AR, Marks RN, Mackay K, Friend RH, Burns PL, Holmes AB. Light-emitting diodes based on conjugated polymers. Nature 1990;347:539–41.
[3] Grimsdale AC, Chan KL, Martin RE, Jokisz PG, Holmes AB. Synthesis of light-emitting conjugated polymers for applications in electroluminescent devices. Chem Rev 2009;109:897–1091.
[4] Akcelrud L. Electroluminescent polymers. Prog Polym Sci 2003;28:875–962.
[5] Kim DY, Cho HN, Kim CY. Blue light emitting polymers. Prog Polym Sci 2000;25:1089–139.
[6] Shimizu M, Hiyama T. Organic fluorophores exhibiting highly efficient photoluminescence in the solid state. Chem Asian J 2010;5:1516–31.
[7] Samuel IDW, Turnbull GA. Organic semiconductor lasers. Chem Rev 2007;107:1272–97.
[8] McGehee MD, Heeger AJ. Semiconducting (conjugated) polymers as materials for solid-state lasers. Adv Mater 2000;12:1655–68.
[9] Kozlov VG, Forrest SR. Lasing action in organic semiconductor thin films. Curr Opin Solid State Mater Sci 1999;4:203–8.
[10] Feng X, Liu L, Wang S, Zhu D. Water-soluble fluorescent conjugated polymers and their interactions with biomacromolecules for sensitive biosensors. Chem Soc Rev 2010;39:2411–9.
[11] Wang M, Zhang GX, Zhang DQ, Zhu DB, Tang BZ. Fluorescent bio/chemosensors based on silole and tetraphenylethene luminogens with aggregation-induced emission feature. J Mater Chem 2010;20:1858–67.
[12] Gonçalves MST. Fluorescent labeling of biomolecules with organic probes. Chem Rev 2009;109:190–212.
[13] Frommer WB, Davidson MW, Campbell RE. Genetically encoded biosensors based on engineered fluorescent proteins. Chem Soc Rev 2009;38:2833–41.
[14] Basabe-Desmonts L, Reinhoudt DN, Crego-Calama M. Design of fluorescent materials for chemical sensing. Chem Soc Rev 2007;36:993–1017.
[15] Thomas III SW, Joly GD, Swager TM. Chemical sensors based on amplifying fluorescent conjugated polymers. Chem Rev 2007;107:1339–86.
[16] Adhikari B, Majumdar S. Polymers in sensor applications. Prog Polym Sci 2004;29:699–766.
[17] Figueira TM, Rosso PGD, Trattnig R, Sax S, List EJW, Müllen K. Designed suppression of aggregation in polypyrene: toward high-performance blue-light-emitting diodes. Adv Mater 2010;22:990–3.
[18] Shiraishi K, Kashiwabara T, Sanji T, Tanaka M. Aggregation-induced emission of dendritic phosphole oxides. New J Chem 2009;33:1680–4.
[19] Miyake J, Chujo Y. Thermally stabilized blue luminescent poly(*p*-phenylene)s covered with polyhedral oligomeric silsesquioxanes. Macromol Rapid Commun 2008;29:86–92.
[20] Swager TM. Iptycenes in the design of high performance polymers. Acc Chem Res 2008;41:1181–9.

[21] Satrijo A, Kooi SE, Swager TM. Enhanced luminescence from emissive defects in aggregated conjugated polymers. Macromolecules 2007;40:8833–41.

[22] Zhao CH, Wakamiya A, Yamaguchi S. Highly emissive poly(aryleneethynylene)s containing 2,5-diboryl-1,4-phenylene as a building unit. Macromolecules 2007;40:3898–900.

[23] Amrutha SR, Jayakannan M. Structure control of π-conjugated polymers for enhanced solid-state luminescence: synthesis and liquid crystalline and photophysical properties of new bulky poly(p-phenylenevinylene)s and oligo(phenylenevinylene)s bearing tricyclodecane pendants. Macromolecules 2007;40:2380–91.

[24] Wang J, Zhao Y, Dou YC, Sun H, Xu P, Ye K, Zhang J, Jiang S, Li F, Wang Y. Alkyl and dendron substituted quinacridones: synthesis, structures, and luminescent properties. J Phys Chem B 2007;111:5082–9.

[25] Pu KY, Zhang B, Ma Z, Wang P, Qi XY, Chen RF, Wang LH, Fan QL, Huang W. Synthesis, morphology and photophysics of novel hybrid organic-inorganic polyhedral oligomeric silsesquioxane-tethered poly(fluoreneethynylene). Polymer 2006;47:1970–8.

[26] Wu CW, Tsai CM, Lin HC. Synthesis and characterization of poly(fluorene)-based copolymers containing various 1,3,4-oxadiazole dendritic pendants. Macromolecules 2006;39:4298–305.

[27] Hecht S, Fréchet JMJ. Dendritic encapsulation of function: applying nature's site isolation principle from biomimetic to materials science. Angew Chem Int Ed 2001;40:74–91.

[28] Zhao CH, Sakuda E, Wakamiya A, Yamaguchi S. Highly emissive diborylphenylene-containing bis(phenylethynyl)benzenes: structure-photophysical property correlations and fluoride ion sensing. Chem Eur J 2009;15:10603–12.

[29] Guo CC, Lin CH, Chen WC. Morphology and photophysical properties of light-emitting electrospun nanofibers prepared from poly(fluorene) derivative/PMMA blends. Macromolecules 2007;40:6959–66.

[30] Li C, Liu X, Yuan M, Li J, Guo Y, Xu J, Zhu M, Lv J, Liu H, Li Y. Unusual fluorescence enhancement of a novel carbazolyldiacetylene bound to gold nanoparticles. Langmuir 2007;23:6754–60.

[31] Wu SH, Huang HM, Chen KC, Hu CW, Hsu CC, Tsiang RCC. A green polymeric light-emitting diode materials: poly(9,9-dioctylfluorene-alt-thiophene) end-capped with gold. Adv Funct Mater 2006;15:1959–66.

[32] Nguyen BT, Gautrot JE, Ji C, Brunner PL, Nguyen MT, Zhu XX. Enhancing the photoluminescence intensity of conjugated polycationic polymers by using quantum dots as antiaggregation reagents. Langmuir 2006;22:4799–803.

[33] Kulkarni AP, Jenekhe SA. Blue light-emitting diodes with good spectra stability based on blends of poly(9,9-dioctylfluorene): interplay between morphology, photophysics, and device performance. Macromolecules 2003;36:5285–96.

[34] Gaylord BS, Wang S, Heeger AJ, Bazan GC. Water-soluble conjugated oligomers: effect of chain length and aggregation on photoluminescence-quenching efficiencies. J Am Chem Soc 2001;123:6417–8.

[35] Shimizu M, Takeda Y, Higashi M, Hiyama T. 1,4-bis(alkenyl)-2,5-dipiperidinobenzenes: minimal fluorophores exhibiting highly efficient emission in the solid state. Angew Chem Int Ed 2009;48:3653–6.

[36] Tang WX, Xiang Y, Tong AJ. Salicylaldehyde azines as fluorophores of aggregation-induced emission enhancement characteristics. J Org Chem 2009;74:2163–6.

[37] Wu YT, Kuo MY, Chang YT, Shin CC, Wu TC, Tai CC, Cheng TH, Liu WS. Synthesis, structure, and photophysical properties of highly substituted 8,8a-dihydrocyclopenta[a]indenes. Angew Chem Int Ed 2008;47:9891–4.

[38] Wang M, Zhang DQ, Zhang GX, Zhu DB. The convenient fluorescence turn-on detection of heparin with a silole derivative featuring an ammonium group. Chem Commun 2008:4469–71.

[39] Qian Y, Li S, Zhang G, Wang Q, Wang S, Xu H, Li C, Li Y, Yang G. Aggregation-induced emission enhancement of 2-(2′-hydroxyphenyl)benzothiazole-based excited-state intramolecular proton-transfer compounds. J Phys Chem B 2007;111:5861–8.

[40] Toal SJ, Jones KA, Magde D, Trogler WC. Luminescent silole nanoparticles as chemoselective sensors for Cr(VI). J Am Chem Soc 2005;127:11661–5.

[41] Ning Z, Chen Z, Zhang Q, Yan Y, Qian S, Cao Y, Tian H. Aggregation-induced emission (AIE)-active starburst triarylamine fluorophores as potential non-doped red emitters for organic light-emitting diodes and Cl₂ gas chemodosimeter. Adv Funct Mater 2007;17:3799–807.

[42] Liu Y, Tao X, Wang F, Shi J, Sun J, Yu W, Ren Y, Zou D, Jiang M. Intermolecular hydrogen bonds induced highly emissive excimers: enhancement of solid-state luminescence. J Phys Chem C 2007;111:6544–9.

[43] Chen Y, Lv Y, Han Y, Zhu B, Zhang F, Bo Z, Liu CY. Dendritic effect on supramolecular self-assembly: organogels with strong fluorescence emission induced by aggregation. Langmuir 2009;25:8548–55.

[44] Qian L, Zhi J, Tang B, Yang F, Zhao W, Dong Y. Organic compounds with aggregation-induced emission. Prog Chem 2008;20:673–8.

[45] Zhao Q, Li Lei, Li F, Yu M, Liu Z, Yi T, Huang C. Aggregation-induced phosphorescent emission (AIPE) of iridium(III) complexes. Chem Commun 2008:685–7.

[46] Lee YT, Chiang CL, Chen CT. Solid-state highly fluorescent diphenylaminospirobifluorenylfumaronitrile red emitters for non-doped organic light-emitting diodes. Chem Commun 2008:217–9.

[47] Xie Z, Yang B, Li F, Cheng G, Liu L, Yang G, Xu H, Ye L, Hanif M, Liu S, Ma D, Ma Y. Cross dipole stacking in the crystal of distyrylbenzene derivative: the approach toward high solid-state luminescence efficiency. J Am Chem Soc 2005;127:14152–3.

[48] Han MR, Hirayam Y, Hara M. Fluorescence enhancement from self-assembled aggregates: substituted effects on self-assembly of azobenzenes. Chem Mater 2006;18:2784–6.

[49] An BK, Kwon SK, Jung SD, Park SY. Enhanced emission and its switching in fluorescent organic nanoparticles. J Am Chem Soc 2002;124:14410–5.

[50] Bhongale CJ, Hsu CS. Emission enhancement by formation of aggregates in hybrid chromophoric surfactant amphiphile/silica nanocomposite. Angew Chem Int Ed 2006;45:1404–8.

[51] Bhongale CJ, Chang CW, Lee CS, Diau EWG, Hsu CS. Relaxation dynamics and structural characterization on formation of organic nanoparticles with enhance emission. J Phys Chem B 2005;109:13472–82.

[52] Luo J, Xie Z, Lam JWY, Cheng L, Chen H, Qiu C, Kwok HS, Zhan XW, Liu Y, Zhu D, Tang BZ. Aggregation-induced emission of 1-methyl-1,2,3,4,5-pentaphenylsilole. Chem Commun 2001:1740–1.

[53] Tang BZ, Zhan X, Yu G, Lee PPS, Liu Y, Zhu D. Efficient blue emission from silole. J Mater Chem 2001;11:2974–8.

[54] Fukazawa A, Ichihashi Y, Yamaguchi S. Intense fluorescence of 1-aryl-2,3,4,5-tetraphenylphospole oxides in the crystalline state. New J Chem 2010;34:1537–40.

[55] Lamère JF, Saffon N, Santos ID, Fery-Forgues S. Aggregation-induced emission enhancement in organic ion pairs. Langmuir 2010;26:10210–7.

[56] Kokado K, Nagai A, Chujo Y. Poly(γ-glutamic acid) hydrogels with water-sensitive luminescence derived from aggregation-induced emission of o-carborane. Macromolecules 2010;43:6463–8.

[57] Qian LJ, Tong B, Shen JB, Shi JB, Zhi JG, Dong YQ, Yang F, Dong YP, Lam JWY, Liu Y, Tang BZ. Crystallization-induced emission enhancement in a phosphorus-containing heterocyclic luminogen. J Phys Chem B 2009;113:9098–103.

[58] Zheng YS, Hu YJ. Chiral recognition based on enantioselectively aggregation-induced emission. J Org Chem 2009;74:5660–3.

[59] Zheng YS, Hu YJ, Li DM, Chen YC. Enantiomer analysis of chiral carboxylic acids by AIE molecules bearing optically pure aminol groups. Talanta 2010;80:1470–4.

[60] An P, Shi ZF, Dou W, Cao XP, Zhang HL. Synthesis of 1,4-bis[2,2-bis(4-alkoxyphenyl)vinyl]benzenes and side chain modulation of their solid-state emission. Org Lett 2010;12:4364–7.

[61] Chen XT, Xiang Y, Li N, Song PS, Tong AJ. Fluorescence turn-on detection of protamine based on aggregation-induced emission enhancement characteristics of 4-(6′-carboxyl) hexyloxysalicylaldehyde azine. Analyst 2010;135:1098–105.

[62] Chen J, Law CCW, Lam JWY, Dong Y, Lo SMF, Williams ID, Zhu D, Tang BZ. Synthesis, light emission, nanoaggregation, and restriction intramolecular rotation of 1,1-substituted 2,3,4,5-tetraphenylsiloles. Chem Mater 2003;15:1535–46.

[63] Li K, Liu B. Water-soluble conjugated polymers as the platform for protein sensors. Polym Chem 2010;1:252–9.

[64] Jo J, Lee D. Turn-on fluorescence detection of cyanide in water: activation of latent fluorophores through remote hydrogen bonds that mimic peptide b-turn motif. J Am Chem Soc 2009;131:16283–91.

[65] Zeng Q, Zhang L, Li Z, Qin J, Tang BZ. New polyacetylene-based chemosensory materials for the turn-on sensing of α-amino acids. Polymer 2009;50:434–40.

[66] Germain ME, Knapp MJ. Optical explosives detection: from color changes to fluorescence turn-on. Chem Soc Rev 2009;38:2543–55.

[67] Gao BR, Wang HY, Hao YW, Fu LM, Fang HH, Jiang Y, Wang L, Chen QD, Xia H, Pan LY, Ma YG, Sun HB. Time-resolved fluorescence study of aggregation-induced emission enhancement by restriction of intramolecular charge transfer state. J Phys Chem B 2010;114:128–34.

[68] Qin A, Lam JWY, Mahtab F, Jim CKW, Tang L, Sun J, Sung HHY, Williams ID, Tang BZ. Pyrazine lumiogens with "free" and "locked" phenyl rings: understanding of restriction of intramolecular rotation as a cause for aggregation-induced emission. Appl Phys Lett 2009;94:253308.

[69] Liu J, Lam JWY, Tang BZ. Aggregation-induced emission of silole molecules and polymers: fundamental and applications. J Inorg Organomet Polym 2009;19:249–85.

[70] He J, Xu B, Chen F, Xia H, Li K, Ye L, Tian W. Aggregation-induced emission in the crystals of 9,10-distyrylanthracene derivatives: the essential role of restricted intramolecular torsion. J Phys Chem C 2009;113:9892–9.

[71] Tong H, Dong YQ, Hong Y, Häußler M, Lam JWY, Sung HHY, Yu X, Sun J, Williams ID, Kwok HS, Tang BZ. Aggregation-induced emission: effects of molecular structure, solid-state conformation, and morphological packing arrangement on light-emitting behaviors of diphenyldibenzofulvene derivatives. J Phys Chem C 2007;111:2287–94.

[72] Yu G, Yin S, Liu YQ, Chen J, Xu X, Sun X, Ma D, Zhan X, Peng Q, Shuai ZG, Tang BZ, Zhu D, Fang W, Luo Y. Structures, electronic states, photoluminescence, and carrier transport properties of 1,1-disubstituted 2,3,4,5-tetraphenylsiloles. J Am Chem Soc 2005;127:6335–46.

[73] Li Z, Dong YQ, Mi B, Tang YH, Häußler M, Tong H, Dong YP, Lam JWY, Ren Y, Sung HHY, Wong KS, Gao P, Williams ID, Kwok HS, Tang BZ. Structural control of the photoluminescence of silole regioisomers and their utility as sensitive regiodiscriminating chemosensors and efficient electroluminescent materials. J Phys Chem B 2005;109:10061–6.

[74] Ren Y, Lam JWY, Dong YQ, Tang BZ, Wong KS. Enhanced emission efficiency and excited state lifetime due to restricted intramolecular motion in silole aggregates. J Phys Chem B 2005;109: 1135–40.

[75] Park C, Hong JI. A new fluorescent sensor for the detection of pyrophosphate based on a tetraphenylethylene moiety. Tetrahedron Lett 2010;51:1960–2.

[76] Wang W, Lin T, Wang M, Liu TX, Ren L, Chen D, Huang S. Aggregation emission properties of oligomers based on tetraphenylethylene. J Phys Chem B 2010;114:5983–8.

[77] Xue W, Zhang G, Zhang D, Zhu D. A new label-free continuous fluorometric assay for trypsin and inhibitor screening with tetraphenylethene compounds. Org Lett 2010;12: 2274–7.

[78] Liu Y, Tang Y, Barashkov NN, Irgibaeva IS, Lam JWY, Hu R, Birimzhanova D, Yu Y, Tang BZ. Fluorescent chemosensor for detection and quantitation of carbon dioxide gas. J Am Chem Soc 2010;132:13951–3.

[79] Hong YN, Lam JWY, Tang BZ. Aggregation-induced emission: phenomenon, mechanism and applications. Chem Commun 2009:4332–53.

[80] Lo SC, Burn PL. Development of dendrimers: macromolecules for use in organic light-emitting diodes and solar cells. Chem Rev 2007;107:1097–116.

[81] Shirakawa H. The discovery of polyacetylene film: the dawning of an era of conducting polymers. Angew Chem Int Ed 2001;40:2575–80 [Nobel Lecture].

[82] MacDiarmid AG. "Synthetic metals": a novel role for organic polymers. Angew Chem Int Ed 2001;40:2581–90 [Nobel Lecture].

[83] Heeger AJ. Semiconducting and metallic polymers: the fourth generation of polymeric materials. Angew Chem Int Ed 2001;40:2591–611 [Nobel Lecture].

[84] Akagi K. Helical polyacetylene: asymmetric polymerization in a chiral liquid-crystal field. Chem Rev 2009;109:5354–401.

[85] Masuda T. Substituted polyacetylenes. J Polym Sci Part A Polym Chem 2007;45:165–80.

[86] Huang CH, Yang SH, Chen KB, Hsu CS. Synthesis and light emitting properties of polyacetylenes having pendent fluorene groups. J Polym Sci Part A Polym Chem 2006;44:519–31.

[87] Liu JZ, Lam JWY, Tang BZ. Acetylene polymers: syntheses, structures, and functions. Chem Rev 2009;109:5799–867.

[88] Lam JWY, Tang BZ. Functional polyacetylenes. Acc Chem Res 2005;38:745–54.

[89] Lam JWY, Tang BZ. Liquid-crystalline and light-emitting polyacetylenes. J Polym Sci Part A Polym Chem 2003;41:2607–29.

[90] Lee WE, Kim JW, Oh CJ, Sakaguchi T, Fujiki M, Kwak G. Correlation of intramolecular excimer emission with lamellar layer distance in liquid-crystalline polymers: verification by the film-swelling method. Angew Chem Int Ed 2010;49:1406–9.

[91] Yanari SS, Bovey FA, Lumry R. Fluorescence of styrene homopolymers and copolymers. Nature 1963;200:242–4.

[92] Qin AJ, Jim CKW, Tang YH, Lam JWY, Liu JZ, Mahtab F, Gao P, Tang BZ. Aggregation-enhanced emissions of intramolecular excimers in disubstituted polyacetylenes. J Phys Chem B 2008;112:9281–8.

[93] Yuan WZ, Qin AJ, Lam JWY, Sun JZ, Dong YQ, Häussler M, Liu JZ, Xu HP, Zheng Q, Tang BZ. Disubstituted polyacetylenes containing photopolymerizable vinyl groups and polar ester functionality: polymer synthesis, aggregation-enhanced emission, and fluorescent pattern formation. Macromolecules 2007;40:3159–66.

[94] Jim CKW, Qin AJ, Lam JWY, Häussler M, Tang BZ. Aggregation-induced emission enhancement of polyacetylenes. Polym Mater Sci Eng 2007;96:414–5.

[95] Chen JW, Xie ZL, Lam JWY, Law CCW, Tang BZ. Silole-containing polyacetylenes. Synthesis, thermal stability, light emission, nanodimensional aggregation, and restricted intramolecular rotation. Macromolecules 2003;36:1108–17.

[96] Yuan WZ, Zhao H, Shen XY, Mahtab F, Lam JWY, Sun JZ, Tang BZ. Luminogenic polyacetylenes and conjugated polyelectrolytes: synthesis, hybridization with carbon nanotubes, aggregation-induced emission, superamplification in emission quenching by explosives, and fluorescent assay for protein quantitation. Macromolecules 2009;42:9400–11.

[97] Pu KY, Cai L, Liu B. Design and synthesis of charge-transfer-based conjugated polyelectrolytes as multicolor light-up probes. Macromolecules 2009;42:5933–40.

[98] Pu KY, Liu B. Conjugated polyelectrolytes as light-up macromolecular probes for heparin sensing. Adv Funct Mater 2009;19:277–84.

[99] Tong H, Hong Y, Dong Y, Häussler M, Lam JWY, Li Z, Guo Z, Guo Z, Tang BZ. Fluorescent "light-up" bioprobes based on tetraphenylethylene derivatives with aggregation-induced emission characteristics. Chem Commun 2006:3705–7.

[100] Liu B, Bazan GC. Homogeneous fluorescence-based DNA detection with water-soluble conjugated polymers. Chem Mater 2004;16:4467–76.

[101] Voit BI, Lederer A. Hyperbranched and highly branched polymer architectures-synthetic strategies and major characterization aspects. Chem Rev 2009;109:5924–73.

[102] Qin A, Lam JWY, Dong H, Lu W, Jim CKW, Dong YQ, Häußler M, Sung HHY, Williams ID, Wong GKL, Tang BZ. Metal-free, regioselective diyne polycyclotrimerization: synthesis, photoluminescence, solvatochromism, and two-photon absorption of a triphenylamine-containing hyperbranched poly(aroylarylene). Macromolecules 2007;40:4879–86.

[103] Gao C, Yan D. Hyperbranched polymers: from synthesis to applications. Prog Polym Sci 2004;29:183–275.

[104] Häußler M, Qin A, Tang BZ. Acetylenes with multiple triple bonds: a group of versatile A_n-type building blocks for the construction of functional hyperbranched polymers. Polymer 2007;48: 6181–204.

[105] Häußler M, Tang BZ. Functional hyperbranched macromolecules constructed from acetylenic triple-bond building blocks. Adv Polym Sci 2007;209:1–58.

[106] Chen JW, Peng H, Law CCW, Dong YP, Lam JWY, Williams ID, Tang BZ. Hyperbranched poly(phenylenesilolene)s: synthesis, thermal stability, electronic conjugation, optical power limiting, and cooling-enhanced light emission. Macromolecules 2003;36:4319–27.

[107] Liu JZ, Zhong YC, Lam JWY, Lu P, Hong YN, Yu Y, Yue YN, Faisal M, Sung HHY, Williams ID, Wong KS, Tang BZ. Hyperbranched conjugated polysiloles: synthesis, structure, aggregation-enhanced emission, multicolor fluorescent photopatterning, and super-amplified detection of explosives. Macromolecules 2010;43: 4921–36.

[108] Liu JZ, Zheng RH, Tang YH, Häussler M, Lam JWY, Qin AJ, Ye MX, Hong YN, Gao P, Tang BZ. Hyperbranched poly(silylenephenylenes from polycyclotrimerization of A_2-type diyne monomers: synthesis, characterization, structural modeling, thermal stability, and fluorescent patterning. Macromolecules 2007;40:7473–86.

[109] Liu JZ, Zhong YC, Lu P, Hong YN, Lam JWY, Faisal M, Yu Y, Wong KS, Tang BZ. A superamplification effect in the detection of explosives by a fluorescent hyperbranched poly(silylenephenylene) with aggregation-enhanced emission characteristics. Polym Chem 2010;1:426–9.

[110] Zeng Q, Li Z, Dong YQ, Di CA, Qin AJ, Hong YN, Ji L, Zhu ZC, Jim CKW, Yu G, Li QQ, Li ZA, Liu YQ, Qin JG, Tang BZ. Fluorescence enhancements of benzene-cored luminophores by restricted intramolecular rotations: AIE and AIEE effects. Chem Commun 2007:70–2.

[111] Lu P, Lam JWY, Liu J, Jim CKW, Yuan W, Xie N, Zhong Y, Hu Q, Wong KS, Cheuk KKL, Tang BZ. Aggregation-induced emission in a hyperbranched poly(silylenevinylene) and superamplification in its emission quenching by explosive. Macromol Rapid Commun 2010;31:834–9.

[112] Rostovtsev VV, Green LG, Fokin VV, Sharpless KB. A stepwise Huisgen cycloaddition process: copper(I)-catalyzed regioselective "ligation" of azides and terminal alkynes. Angew Chem Int Ed 2002;41:2596–9.

[113] Tornøe CW, Christensen C, Meldal M. Peptidotriazoles on solid phase: [1,2,3]-triazoles by regiospecific copper(I)-catalyzed 1,3-dipolar cycloadditions of terminal alkynes to azides. J Org Chem 2002;67:3057–64.

[114] Meldal M, Tornøe CW. Cu-catalyzed azide-alkyne cycloaddition. Chem Rev 2008;108:2952–3015.

[115] Iha RK, Wooley KL, Nyström AM, Burke DJ, Kade MJ, Hawker CJ. Applications of orthogonal "click" chemistries in the synthesis of functional soft materials. Chem Rev 2009;109:5620–86.

[116] Golas PL, Matyjaszewski K. Marrying click chemistry with polymerization: expanding the scope of polymeric materials. Chem Soc Rev 2010;39:1338–54.

[117] Sumerlin BS, Vogt AP. Macromolecular engineering through click chemistry and other efficient transformations. Macromolecules 2010;43:1–13.

[118] Bingder WH, Sachsenhofer R. "Click" chemistry in polymer and material science: an update. Macromol Rapid Commun 2008;29:952–81.

[119] Qin AJ, Lam JWY, Tang BZ. Click polymerization. Chem Soc Rev 2010;39:2522–44.

[120] Qin AJ, Lam JWY, Tang BZ. Click polymerization: progresses, challenges, and opportunities. Macromolecules 2010;43:8693–702.

[121] Qin AJ, Lam JWY, Jim CKW, Zhang L, Yan JJ, Häußler M, Liu JZ, Dong YQ, Liang DH, Chen EQ, Jia GC, Tang BZ. Hyperbranched polytriazoles: click polymerization, regioisomeric structure, light emission, and fluorescent patterning. Macromolecules 2008;41:3808–22.

[122] Qin AJ, Jim CKW, Lu WX, Lam JWY, Häußler M, Dong YQ, Sung HHY, Williams ID, Wong GKL, Tang BZ. Click polymerization: facile synthesis of functional poly(aroyltriazole)s by metal-free, regioselective 1,3-dipolar polycycloaddition. Macromolecules 2007;40:2308–17.

[123] Qin AJ, Lam JWY, Tang L, Jim CKW, Zhao H, Sun JZ, Tang BZ. Polytriazoles with aggregation-induced emission characteristics: synthesis by click polymerization and application as explosive chemosensors. Macromolecules 2009;42:1421–4.

[124] Dong H, Zheng R, Lam JWY, Häussler M, Qin A, Tang BZ. A new route to hyperbranched macromolecules: syntheses of photosensitive poly(aroylarylene)s via 1,3,5-regioselective polycyclotrimerization of bis(aroylacetylene)s. Macromolecules 2005;38:6328–91.

[125] Qin A, Tang L, Lam JWY, Jim CKW, Yu Y, Zhao H, Sun J, Tang BZ. Metal-free click polymerization: synthesis and photonic properties of poly(aroyltriazole)s. Adv Funct Mater 2009;19:1891–900.

[126] Wang J, Mei J, Yuan W, Lu P, Qin A, Sun J, Ma Y, Tang BZ. Hyperbranched polytriazoles with high molecular compressibility: aggregation-induced emission and superamplified explosive detection. J Mater Chem 2011;21:4056–9.

[127] Xu K, Peng H, Sun Q, Dong Y, Salhi F, Luo J, Chen J, Huang Y, Zhang D, Xu Z, Tang BZ. Polycyclotrimerization of diynes: synthesis and properties of hyperbranched polyphenylenes. Macromolecules 2002;35:5821–34.

[128] Grayson SM, Fréchet JMJ. Divergent synthesis of dendronized poly(p-hydroxystyrene). Macromolecules 2001;34:6542–4.

[129] Hong Y, Lam JWY, Tang BZ. Aggregation-induced emission. Chem Soc Rev 2011, doi:10.1039/c1cs15113d.

[130] Hu R, Maldonado JL, Rodriguez M, Deng C, Jim CKW, Lam JWY, Yuen MMF, Damos-Ortiz G, Tang BZ. One- and two photon excited aggregation-induced emissions of tetraphenylethene derivatives. Polym Prepr Am Chem Soc 2011;52(2).

[131] Kokado K, Chujo Y. Emission via aggregation of alternating polymers with o-carborane and p-phenyleneethynylene sequences. Macromolecules 2009;42:1418–20.

[132] Kokado K, Tokoro Y, Chujo Y. Luminescent and axially chiral π-conjugated polymers linked by carboranes in the main chain. Macromolecules 2009;42:9238–42.

[133] Bunz UHF. Poly(aryleneethynylene)s: syntheses, properties, structures, and applications. Chem Rev 2000;100:1605–44.

[134] Lim CS, Kang DW, Tian YS, Han JH, Hwang HL, Cho BR. Detection of mercury in fish organs with a two-photon fluorescent probe. Chem Commun 2010;46:2388–90.

[135] Wang H, Li Z, Shao P, Qin J, Huang ZL. Two-photon absorption property of a conjugated polymer: influence of solvent and concentration on its property. J Phys Chem B 2010;114:22–7.

[136] Shevyakov SV, Li H, Muthyala R, Asato AE, Croney JC, Jameson DM, Liu RSH. Orbital control of the color and excited state properties of formylated and fluorinated derivatives of azulene. J Phys Chem A 2003;107:3295–9.

[137] Wang F, Han MY, Mya KY, Wang Y, Lai YH. Aggregation-driven growth of size-tunable organic nanoparticles using electronically altered conjugated polymers. J Am Chem Soc 2005;127:10350–5.

[138] Zhao Z, Wang S, Lu P, Chan CYK, Liu D, Lam JWY, Sung HHY, Williams ID, Ma Y, Tang BZ. Structural modulation of solid-State emission of 2,5-bis(trialkylsilylethynyl)-3,4-diphenylsiloles. Angew Chem Int Ed 2009;48:7608–11.

[139] Jang S, Kim SG, Jung D, Kwon H, Song J, Cho S, Ko YC, Sohn H. Aggregation-induced emission enhancement of polysilole nanoaggregates. Bull Korean Chem Soc 2006;27:1965–6.

[140] Sohn H, Huddleston RR, Powell DR, West R, Oka W, Xu Y. An electroluminescent polysilole and some dichlorooligosiloles. J Am Chem Soc 1999;121:2935–6.

[141] Sohn H, Sailor MJ, Magde D, Trogler WC. Detection of nitroaromatic explosives based on photoluminescent polymers containing metalloles. J Am Chem Soc 2003;125:3821–30.

[142] Yang Z, Chi Z, Yu T, Zhang X, Chen M, Xu B, Liu S, Zhang Y, Xu J. Triphenylethylene carbazole derivatives as a new class of AIE materials with strong blue light emission and high glass transition temperature. J Mater Chem 2009;19:5541–6.

[143] Yang ZY, Yu T, Chen MN, Zhang XQ, Wang CC, Xu BJ, Zhou X, Liu SW, Zhang Y, Chi ZG, Xu JR. A monomer and its polymer derived from carbazolyl triphenylethylene with aggregation-induced emission effect characteristics. Acta Polym Sin 2009:560–5.

[144] Chou CA, Chien RH, Lai CT, Hong JL. Complexation of bulky camphorsulfonic acid to enhance emission of organic and polymeric fluorophores with inherent quinoline moiety. Chem Phys Lett 2010;501:80–6.

[145] Tang L, Jin JK, Qin A, Yuan WZ, Mao Y, Mei J, Sun JZ, Tang BZ. Fluorescent thermometer operating in aggregation-induced emission mechanism: probing thermal transitions of PNIPAM in water. Chem Commun 2009:4974–6.

[146] Xing CM, Lam JWY, Qin AJ, Dong YQ, Haussler M, Yang WT, Tang BZ. Unique photoluminescence from nonconjugated alternating copolymer poly[(maleic anhydride)-alt-(vinyl acetate)]. Polym Mater Sci Eng 2007;96:418–9.

[147] Xing CM, Yan WT. A novel, facile method for the preparation of uniform, reactive maleic anhydride/vinyl acetate copolymer micro- and nanospheres. Macromol Rapid Commun 2004;25:1568–74.

[148] Pucci A, Rausa R, Ciardelli F. Aggregation-induced luminescence of polyisobutene succinic anhydrides and imides. Macromol Chem Phys 2008;209:900–6.

[149] Pucci A, Barsocchi C, Rausa R, D'Elia L, Ciardelli F. Alder ene functionalization of polyisobutene oligomer and styrene-butadiene-styrene triblock copolymer. Polymer 2005;46:1497–505.

[150] Moad G. The synthesis of polyolefin graft copolymers by reactive extrusion. Prog Polym Sci 1999;24:81–142.

[151] Lehn J-M. Dynamers: dynamic molecular and supramolecular polymers. Prog Polym Sci 2005;30:814–31.

[152] Ruff Y, Buhler E, Candau SJ, Kesselman E, Talmon Y, Lehn J-M. Glycodynamers: dynamic polymers bearing oligosaccharides residues-generation, structure, physicochemical, component exchange, and lectin binding properties. J Am Chem Soc 2010;132:2573–84.

[153] Ruff Y, Lehn J-M. Glycodynamers: fluorescent dynamic analogues of polysaccharides. Angew Chem Int Ed 2008;47:3556–9.